Design of hot-finished tubular steel members using a stiffness reduction method

Merih Kucukler[a,*], Leroy Gardner[b]

[a]*School of Engineering, University of Warwick, Coventry, CV4 7AL, UK*
[b]*Department of Civil and Environmental Engineering, Imperial College London, London, SW7 2AZ, UK*

Abstract

A stiffness reduction method (SRM) for the design of hot-finished tubular steel members is presented in this paper. Stiffness reduction functions that fully capture the adverse influence of imperfections and plasticity on member stability are developed. The proposed SRM is implemented by (i) reducing the flexural stiffness (EI) of the member using the developed stiffness reduction functions, (ii) performing elastic Linear Buckling Analysis (LBA) and Geometrically Nonlinear Analysis (GNA) of the member with reduced flexural stiffness and (iii) making cross-section strength checks and ensuring that the lowest buckling load amplifier from LBA is greater than or equal to 1.0. Owing to the full allowance for the spread of plasticity, residual stresses and geometrical imperfections through stiffness reduction and instability effects through LBA and GNA, the proposed approach offers an enhanced and more direct assessment of structural behaviour relative to traditional design where structural analysis is accompanied by member design equations, effective lengths and the notional load concept. The proposed method is verified against nonlinear finite element modelling for a large number of tubular steel members. Comparisons of the proposed approach against the methods recommended in the European structural steel design code EN 1993-1-1 for the design of tubular members are also provided.

Keywords: Circular hollow section (CHS); finite element analysis; imperfections; inelastic buckling; rectangular hollow section (RHS); square hollow section (SHS); stiffness reduction

1. Introduction

Tubular steel members are commonly employed in structural applications owing to their efficiency in resisting buckling about both principal axes, high torsional stiffness, which suppresses flexural-torsional instability, and aesthetics. Traditional design methods set out in the current structural steel design specifications [1–3] for tubular steel structures invariably utilise member design equations [4–11] in which checks are performed against internal forces obtained from a structural analysis with the nominal elastic stiffness. However, key behavioural aspects such as (i)

*Corresponding author
Email addresses: merih.kucukler@warwick.ac.uk (Merih Kucukler), leroy.gardner@imperial.ac.uk (Leroy Gardner)

the effect of the development of different extents of plasticity within the members on the internal structural force distribution and (ii) the increased support afforded by neighbouring members remaining largely elastic to those experiencing severe levels of plasticity are generally disregarded, and design equations originally developed for simply-supported members [4–11] are applied to members with other end-support conditions, leading to a decreased level of accuracy.

Recognising the aforementioned limitations of traditional design, Surovek and White [12, 13] proposed a method based on second-order elastic analysis of the structure with reduced stiffness for the consideration of the spread of plasticity on the structural behaviour, eliminating the need for the use of the effective length and notional load concepts in the design. The higher accuracy of the method with respect to the prediction of internal member forces and structural resistance was illustrated. Following minor changes, the method of Surovek and White [12, 13] was included in AISC 360-16 [2], and referred to as the direct analysis method. However, due to the inability of the adopted stiffness reduction scheme to fully consider the adverse influence of plasticity and imperfections on member resistances, the direct analysis method still requires either the use of column buckling checks or explicit modelling of member out-of-straightnesses in the structural analysis. Thus, when column buckling checks are performed, the method does not fully depart from traditional design practice and its shortcomings are partially retained. On the other hand, when member out-of-straightnesses are modelled, these shortcomings are overcome but the determination of appropriate shapes and directions for these imperfections for a structure involving a large number of members under various loading conditions may be a challenging procedure. In addition to the proposal of Surovek-Maleck and White [12, 13], Liew and Tang [14] put forward a refined plastic hinge analysis approach for the analysis and design of tubular structures considering the influence of plasticity by means of stiffness reduction. White [15], Kim and Chen [16], Kim et al. [17], Liew et al. [18], Ziemian and McGuire [19], Landesmann and Batista [20] also utilised stiffness reduction in conjunction with plastic hinge analysis to consider the detrimental influence of the spread of plasticity along the member lengths on the behaviour of steel structures.

To establish an advanced and practical structural steel design approach based on second-order elastic analysis that can be readily carried out using conventional structural analysis software, Kucukler et al. [21, 22] put forward a stiffness reduction method utilising stiffness reduction functions able to consider fully the deleterious influence of the spread of plasticity, member out-of-straightness and residual stresses on the structural response and member strengths unlike the method of [12, 13]. Owing to the full consideration of these adverse effects through the stiffness reduction, the method of [21, 22] only requires cross-section strength checks after the analysis of the structure with reduced stiffness, precluding the need for the modelling of member out-of-straightnesses or using member design equations. Thus, it merges the conventional structural analysis and design stages and offers a very direct means of designing steel structures involving regular or irregular (i.e. nonprismatic, curved) members. The accuracy of the method was verified for a large range of cases [21, 22], but its application is limited to structures comprising I-section members only. Moreover, biaxial bending has not been considered.

To extend the method of Kucukler et al. [21, 22] to tubular structures, a stiffness reduction method for the design of hot-finished tubular steel members is proposed in this paper. Stiffness reduction functions for members with hot-finished circular hollow sections (CHS), square hollow sections (SHS) and rectangular hollow sections (RHS) able to consider fully the deleterious influ-

ence of imperfections and plasticity are developed. Unlike the method of [21, 22], the proposed method involves stiffness reduction functions considering the influence of combined biaxial bending and axial loading, thus enabling its application under this most general loading condition. The proposed methods are applied to hot-finished tubular members with Class 1 and 2 sections and not susceptible to flexural-torsional instabilities. Simplified versions of the proposed stiffness reduction approach with simpler stiffness reduction functions are also put forward. The accuracy of the proposed design method is verified against results generated through nonlinear finite element modelling for various loading conditions, cross-section shapes and member slendernesses.

2. Finite element modelling

To verify the proposed stiffness reduction method (SRM), the results obtained from Geometrically and Materially Nonlinear Analyses with imperfections (GMNIA) of beam finite element models were utilised in this study. The finite element models of the investigated tubular members were created using the finite element analysis software Abaqus [23], employing an elastic-plastic linear Timoshenko beam finite element, referred to as B31 in the Abaqus element library [23], which is able to consider transverse shear deformations. Eighty section points were defined within the CHS (16 around the perimeter and 5 through the thickness), while 114 section points were defined within the SHS and RHS. 100 beam elements were utilised in all the beam element models. Since B31 is a Timoshenko beam element utilising linear interpolation functions, one integration point in the middle of each element was used with the numerical Simpson integration in the element formulations as indicated in the user's manual of Abaqus [23]. The locations of the integration points along the lengths of different beam elements provided in the Abaqus element library can be found in the user's manual of Abaqus [23]. The beam element B31 was also selected in the numerical studies carried out during the development of the beam-column design rules of EN 1993-1-1 [11, 24] and other similar studies [25, 26] with the same number of elements to model each structural steel member. Owing to their computational efficiency, beam finite element models were utilised to simulate the great majority of the tubular members in this study, while shell finite elements were only used to model a series of stocky tubular members subjected to uniform biaxial bending, whose results were employed to derive a stiffness reduction function for bending. In these models, a four-noded reduced integration S4R shell element was used, accounting for finite membrane strains and transverse shear deformations. A tri-linear stress-strain relationship was used in the adopted material model, which is shown in Fig. 1, where E is the Young's modulus, E_{sh} is the strain hardening modulus, f_y and ϵ_y are the yield stress and strain respectively and ϵ_{sh} is the strain value at which strain hardening commences. The parameters f_u and ϵ_u correspond to the ultimate stress and strain values respectively. E_{sh} was assumed to be 2 % of E and ϵ_{sh} was taken as $10\epsilon_y$, conforming to the ECCS recommendations [27], though recently proposed more representative values for these two parameters [28] will be considered in future studies. Grade S235 steel grade was used in all the simulations.

The ECCS residual stress patterns [27] recommended for CHS and SHS/RHS, illustrated in Fig. 2 (a) and (b) respectively, were used to define the initial stress values at the integration points through the SIGINI subroutine [23]. The lowest buckling modes of the member about both the principal axes of the cross-section were used to define geometrical imperfections, whose maximum

amplitudes were scaled to the member length L over 1000 (i.e. $L/1000$), as shown in Fig. 3.

3. Stiffness reduction functions

In this section, stiffness reduction functions for tubular steel members are developed. These stiffness reduction functions will be utilised in the implementation of the proposed stiffness reduction method (SRM) in the following sections.

3.1. Stiffness reduction function for axial loading τ_N

The stiffness reduction function for axial loading τ_N is given by the expression below:

$$\tau_N = \frac{4\psi^2}{\alpha^2 N_{Ed}/N_{pl}\left[1+\sqrt{1-4\psi\frac{N_{Ed}/N_{pl}-1}{\alpha^2 N_{Ed}/N_{pl}}}\right]^2} \quad \text{but} \quad \tau_N \leq 1$$
$$\text{where} \quad \psi = 1 + 0.2\alpha\frac{N_{Ed}}{N_{pl}} - \frac{N_{Ed}}{N_{pl}}, \tag{1}$$

where N_{Ed} is the applied axial loading, N_{pl} is the axial yield load equal to the cross-sectional area A multiplied by the yield stress f_y (i.e. $N_{pl} = Af_y$), and α is the imperfection factor taken equal to 0.21 (i.e. $\alpha = 0.21$) in accordance with EN 1993-1-1 [1], in which the use of the column buckling curve 'a' for hot-finished tubular steel members is recommended. It should be noted that the reduction of the flexural stiffnesses of a member about the principal axes with τ_N, whose derivation is described in detail by [21], and performing the Linear Buckling Analysis (LBA) of the member with this reduced flexural stiffness provides an exact match to the EN 1993-1-1 [1] column buckling curves, when the lowest buckling load amplifier α_{cr} from LBA is equal to unity (i.e. $\alpha_{cr} = 1.0$).

3.2. Stiffness reduction function for bending τ_M

In this subsection, stiffness reduction functions for tubular sections under bending τ_M are calibrated considering moment-curvature $M_{Ed} - \varphi$ responses obtained from GMNIA of shell finite element models of stocky beams subjected to uniform bending with a series of CHS, SHS and RHS. In total, 10 CHS and 20 SHS/RHS subjected to monoaxial bending were considered, while CHS 114.3 × 3.6, SHS 100 × 5 and RHS 200 × 100 × 8 sections were subjected biaxial bending considering various ratios between the bending moments about the y and z principal axes, i.e. $M_{y,Ed}$ and $M_{z,Ed}$ respectively. Note that in the case of CHS, there are no definitive y and z principal axes unlike RHS. However, since the proposed SRM will be extended to space frames involving CHS members in future work, the stiffness reduction patterns of CHS with respect to the orthogonal global axes of a frame are necessary for the implementation of the SRM. The range of the geometrical properties of the considered cross-sections subjected to monoaxial bending is provided in Table 1, where t is the thickness, d is the diameter of the CHS and b and h are the cross-section width and depth of SHS/RHS respectively (see Fig. 2 for the properties with respect to the principal y and z axes).

3.2.1. Stiffness reduction function for bending about the principal y axis τ_{My}

As shown in Fig. 4, to derive a stiffness reduction function from GMNIA for bending about the major axis τ_{My}, secant flexural stiffnesses about the major axis $EI_{s,y}$ were initially determined by dividing the applied bending moment $M_{y,Ed}$ by the corresponding curvatures φ_y of the beams considering various ratios between the bending moments applied about the y and z principal axes η_{zy}, i.e. $EI_{s,y} = M_{y,Ed}/\varphi_y$. The simultaneously applied bending moments $M_{y,Ed}$ and $M_{z,Ed}$ were varied from zero to the full utilisation of the cross-sections under biaxial bending, and the ratios of bending moments applied about the y and z principal axes $\eta_{zy} = M_{z,Ed}/M_{y,Ed}$ were varied from zero to ten. Division of the secant stiffnesses $EI_{s,y}$ by the initial elastic flexural stiffness EI_y provided the stiffness reduction function for bending about the y principal axis τ_{My} (i.e. $\tau_{My} = EI_{s,y}/EI$). The stiffness reduction function obtained by calibration to the GMNIA results is as follows:

$$\begin{aligned}
\tau_{My} &= 1.0 \quad \text{if} \quad M_{y,Ed}/M_{y,pl} \le \phi_y, \\
\tau_{My} &= \tau_{Mly} + (1-\tau_{Mly})\left[1 - \left(\frac{M_{y,Ed}/M_{y,pl} - \phi_y}{\xi_{my} - \phi_y}\right)^{\beta_{my}}\right]^{1/\beta_{my}} \quad \text{if} \quad \phi_y \le M_{y,Ed}/M_{y,pl} \le \xi_{my}, \\
\tau_{My} &= \tau_{Mly}\left[1 - \left(\frac{M_{y,Ed}/M_{y,pl} - \xi_{my}}{m_{ry} - \xi_{my}}\right)\right]^{1/\delta_{my}} \quad \text{if} \quad \xi_{my} \le M_{y,Ed}/M_{y,pl},
\end{aligned} \tag{2}$$

where $M_{y,Ed}$ and $M_{z,Ed}$ are the applied bending moments about the y and z axes respectively, $M_{y,pl}$ is plastic bending moment resistance about the principal y axis equal to the plastic section modulus about this axis multiplied by the yield stress (i.e. $M_{y,pl} = W_{pl,y}f_y$), η_{zy} is the ratio of bending moment applied about the z principal axis to that applied about the y principal axis (i.e. $\eta_{zy} = M_{z,Ed}/M_{y,Ed}$), and τ_{Mly}, ϕ_y, ξ_{my}, β_{my} and δ_{my} are auxiliary coefficients calibrated to GMNIA results, whose values are provided in Table 2. Note that the y and z principal axes correspond to the major and minor axes respectively for the RHS.

As can be seen in Fig. 4, the higher the n_{zy} value, the higher the rate of stiffness reduction. Fig. 4 shows that the stiffness reduction patterns obtained from GMNIA exhibit three distinct stages with respect to the development of plasticity: (i) the elastic stage, where the cross-section remains fully elastic, (ii) the primary plastic stage, where the cross-section experiences a slow rate of secant stiffness reduction following the onset and initial spread of plasticity, and finally (iii) the secondary plastic stage where the cross-section undergoes a more rapid rate of stiffness loss due to the further spread of plasticity. The stiffness reduction function for bending τ_{My} provided by eq. (2) involves three discrete parts representing these three stages, in which the auxiliary coefficient ϕ_y corresponds to the bending moment value at the onset of yielding (i.e. the onset of the primary plastic stage), ξ_y and $\tau_{Ml,y}$ represent the bending moment value and stiffness reduction rate at the beginning of the secondary plastic stage, and finally m_{ry} represents the normalised plastic bending moment resistance of the cross-section about the principal y axis reduced due to the presence of bending moment about the principal z axis.

It should be noted that the values of the auxiliary coefficients τ_{Mly}, β_{my}, δ_{my} in Table 2, which were used in τ_{My} considering the stiffness reduction functions developed by Zubydan [29], were determined such that the coefficient of variation (COV) of the ratios of the stiffness reduction factors predicted by eq. (2) to those obtained from the GMNIA was minimised with the average of

these ratios close to 1.0. Moreover, ξ_{my} corresponding to the normalised bending moment value at the beginning of the secondary plastic stage is expressed by multiplying the normalised bending moment resistance of the cross-section m_{ry} reduced due to the presence of minor axis bending by a factor; this factor was calibrated as 1/1.4 for CHS, $0.89(h/b)^{-0.05}$ for RHS and 0.89 for SHS, thereby leading to a minimum COV of the ratios of the stiffness reduction factors determined by eq. (2) to those obtained from GMNIA. The parameter ϕ_y within τ_{My}, corresponding to the major axis bending moment at which yielding starts $M_{y,Ed,yield}$ normalised by the major axis plastic bending moment resistance $M_{y,pl}$ (i.e. $\phi_y = M_{y,Ed,yield}/M_{y,pl}$), was analytically determined considering the first yield condition of the cross-section through the following equations for RHS, where the minor axis bending moment at the first yield is defined as $M_{z,Ed,yield}$ and the maximum residual stress is equal to $f_{res,max} = 0.5f_y$ as shown in Fig. 2:

$$\begin{aligned} \frac{M_{y,Ed,yield}}{W_{el,y}} + \frac{M_{z,Ed,yield}}{W_{el,z}} &= f_y - f_{res,max} \\ \frac{M_{y,Ed,yield}}{W_{pl,y}f_y}\frac{W_{pl,y}}{W_{el,y}}\left(1 + \eta_{zy}\frac{W_{el,y}}{W_{el,z}}\right) &= 1 - f_{res,max}/f_y \\ f_{res,max} = 0.5f_y \qquad \phi_y = \frac{M_{y,Ed,yield}}{W_{pl,y}f_y} &= \frac{0.5W_{el,y}}{W_{pl,y}\left(1 + \eta_{zy}\frac{W_{el,y}}{W_{el,z}}\right)}. \end{aligned} \tag{3}$$

Since the sections are assumed to be proportionally loaded:

$$\eta_{zy} = \frac{M_{z,Ed}}{M_{y,Ed}} = \frac{M_{z,Ed,yield}}{M_{y,Ed,yield}}. \tag{4}$$

Note that for SHS and RHS, the maximum normal stresses resulting from the bending moments plus residual stresses are at the corners. Also, for SHS, since $W_{el,y} = W_{el,z}$, the expression of ϕ_y simplifies to

$$\phi_y = \frac{M_{y,Ed,yield}}{W_{pl,y}f_y} = \frac{0.5W_{el,y}}{W_{pl,y}\left(1 + \eta_{zy}\right)}. \tag{5}$$

For circular hollow sections (CHS), ϕ_y was determined by taking the resultant of the bending moments applied about the y and z axes $\sqrt{M^2_{y,Ed,yield} + M^2_{z,Ed,yield}}$, assuming the first yield condition and considering a maximum residual stress of $f_{res,max} = 0.15f_y$ (see Fig. 2) through the following equations:

$$\begin{aligned} \frac{\sqrt{M^2_{y,Ed,yield} + M^2_{z,Ed,yield}}}{W_{el,y}} = \frac{M_{y,Ed,yield}\sqrt{1 + \eta^2_{zy}}}{W_{el,y}} &= f_y - f_{res,max} \\ \frac{M_{y,Ed,yield}}{f_y W_{pl,y}}\frac{W_{pl,y}}{W_{el,y}}\sqrt{1 + \eta^2_{zy}} &= 1 - f_{res,max}/f_y \\ f_{res,max} = 0.15f_y \qquad \phi_y = \frac{M_{y,Ed,yield}}{W_{pl,y}f_y} &= \frac{0.85W_{el,y}}{W_{pl,y}\sqrt{1 + \eta^2_{zy}}}. \end{aligned} \tag{6}$$

Finally, the coefficients m_{ry} in Table 2, corresponding to the major axis bending moment resistance of the cross-section reduced due to the presence of minor axis bending $M_{y,Ed,max}$ and normalised by $M_{y,pl}$ (i.e. $m_{ry} = M_{y,Ed,max}/M_{y,pl}$), were determined using the ultimate cross-section strength equations put forward by Duan and Chen [30] for tubular sections under biaxial bending, which are provided below for SHS and RHS:

$$\left(\frac{M_{y,Ed}}{M_{y,pl}}\right)^{1.7} + \left(\frac{M_{z,Ed}}{M_{z,pl}}\right)^{1.7} \leq 1.0, \tag{7}$$

and for CHS:

$$\left(\frac{M_{y,Ed}}{M_{y,pl}}\right)^{2} + \left(\frac{M_{z,Ed}}{M_{z,pl}}\right)^{2} \leq 1.0. \tag{8}$$

The normalised major axis bending moment resistance $m_{ry} = M_{y,Ed,max}/M_{y,pl}$ for SHS and RHS was determined using eq. (7) as follows, where the applied minor axis bending moment also assumes its maximum value $M_{z,Ed,max}$:

$$\begin{aligned}
\left(\frac{M_{y,Ed,max}}{M_{y,pl}}\right)^{1.7}\left[1 + \left(\frac{M_{z,Ed,max}}{M_{z,pl}}\frac{M_{y,pl}}{M_{y,Ed,max}}\right)^{1.7}\right] &= 1.0 \\
m_{ry}^{1.7}\left[1 + \left(\eta_{zy}\frac{W_{y,pl}}{W_{z,pl}}\right)^{1.7}\right] &= 1.0 \\
m_{ry} &= \left[\frac{1}{1 + \left(\frac{\eta_{zy}W_{pl,y}}{W_{pl,z}}\right)^{1.7}}\right]^{1/1.7}.
\end{aligned} \tag{9}$$

Note that since the sections are assumed to be proportionally loaded:

$$\eta_{zy} = \frac{M_{z,Ed}}{M_{y,Ed}} = \frac{M_{z,Ed,max}}{M_{y,Ed,max}} \tag{10}$$

Considering $W_{pl,y} = W_{el,y}$, m_{ry} simplifies to the following expression for SHS:

$$m_{ry} = \left[\frac{1}{1 + \eta_{zy}^{1.7}}\right]^{1/1.7}. \tag{11}$$

Following the same procedure adopted for the determination of $m_{ry} = M_{y,Ed,max}/M_{y,pl}$ for SHS and RHS, the reduced, normalised bending moment resistance of CHS was determined using eq. (8) and considering $M_{y,pl} = M_{z,pl}$:

$$\begin{aligned}
\left(\frac{M_{y,Ed,max}}{M_{y,pl}}\right)^{2}\left[1 + \left(\frac{M_{z,Ed,max}}{M_{z,pl}}\frac{M_{y,pl}}{M_{y,Ed,max}}\right)^{2}\right] &= 1.0 \\
m_{ry}^{2}\left(1 + \eta_{zy}^{2}\right) &= 1.0 \\
m_{ry} &= \frac{1}{\sqrt{1 + \eta_{zy}^{2}}}.
\end{aligned} \tag{12}$$

3.2.2. Stiffness reduction function for bending about the principal z axis τ_{Mz}

The stiffness reduction function for bending about the principal z axis is given by:

$$\begin{aligned}
\tau_{Mz} &= 1.0 \quad \text{if} \quad M_{z,Ed}/M_{z,pl} \leq \phi_z, \\
\tau_{Mz} &= \tau_{Mlz} + (1-\tau_{Mlz})\left[1-\left(\frac{M_{z,Ed}/M_{z,pl}-\phi_z}{\xi_{mz}-\phi_z}\right)^{\beta_{mz}}\right]^{1/\beta_{mz}} \quad \text{if} \quad \phi_z \leq M_{z,Ed}/M_{z,pl} \leq \xi_{mz}, \\
\tau_{Mz} &= \tau_{Mlz}\left[1-\left(\frac{M_{z,Ed}/M_{z,pl}-\xi_{mz}}{m_{rz}-\xi_{mz}}\right)\right]^{1/\delta_{mz}} \quad \text{if} \quad \xi_{mz} \leq M_{z,Ed}/M_{z,pl},
\end{aligned} \tag{13}$$

where $\eta_{yz} = M_{y,Ed}/M_{z,Ed}$, $M_{z,pl}$ is the plastic bending moment resistance about the principal z axis determined by multiplying the plastic section modulus about this axis $W_{pl,z}$ by the yield stress f_y (i.e. $M_{z,pl} = W_{pl,z}f_y$). τ_{Mlz}, ϕ_z, ξ_{mz}, β_{mz} and δ_{mz} are auxiliary coefficients calibrated to GMNIA results whose values are provided in Table 3. The same approach described for the determination and calibration of τ_{Mly}, ϕ_y, ξ_{my}, β_{my} and δ_{my} in the previous subsection were followed in the determination and calibration of τ_{Mlz}, ϕ_z, ξ_{mz}, β_{mz} and δ_{mz}, with τ_{Mz} also adopting the same three stage format. A comparison of the calibrated stiffness reduction functions about the y and z principal axes, τ_{My} and τ_{Mz}, against the results obtained from GMNIA are illustrated in Fig. 5 for a CHS 114.3 × 3.6, an SHS 100 × 100 × 5 and an RHS 200 × 100 × 10, showing that the calibrated τ_{My} and τ_{Mz} functions are able to capture very accurately the flexural stiffness degradation of sections under biaxial bending with different ratios between the moments applied about the y and z principal axes (i.e. $\eta_{zy} = M_{z,Ed}/M_{y,Ed}$ and $\eta_{yz} = M_{y,Ed}/M_{z,Ed}$).

3.3. Stiffness reduction function for combined axial loading and bending τ_{MN}

To develop stiffness reduction functions for combined axial loading and bending about the y and z principal axes, which are denoted τ_{MNy} and τ_{MNz} respectively, the stiffness reduction functions developed for axial loading τ_N and bending about the principal axes τ_{My} and τ_{My} were utilised. The following stiffness reduction function applies for the reduction of the flexural stiffness about the principal y axis (i.e. EI_y) of the member under combined axial loading and bending:

$$\tau_{MNy} = \tau_{My}\tau_N\left\{1-\left(\frac{N_{Ed}}{N_{pl}}\right)^{\eta_y}\left(\frac{M_{y,Ed}}{M_{y,pl}}\right)^{\rho_y}\right\}, \tag{14}$$

while the flexural stiffness about the principal z axis (i.e. EI_z) of the member under axial loading plus bending should be reduced through the following stiffness reduction function:

$$\tau_{MNz} = \tau_{Mz}\tau_N\left\{1-\left(\frac{N_{Ed}}{N_{pl}}\right)^{\eta_z}\left(\frac{M_{z,Ed}}{M_{z,pl}}\right)^{\rho_z}\right\}. \tag{15}$$

In eq. (14) and eq. (15), η_y, η_z, ρ_y and ρ_z are auxiliary coefficients provided in Table 4 for CHS, SHS and RHS, obtained through calibration to the GMNIA ultimate strength predictions of beam-columns subjected to uniform bending plus axial compression. It should be noted that following the approach adopted by Kucukler et al. [21], the calibration of η_y and ρ_y for τ_{MNy} and that of η_z and ρ_z for τ_{MNz} was carried out such that the coefficient of variation of the ratios of the ultimate

axial load carrying capacities obtained through the SRM to those obtained through GMNIA was minimised for beam-columns subjected to axial loading plus bending. As can be seen from eq. (14) and eq. (15), the proposed stiffness reduction functions τ_{MNy} and τ_{MNz} degenerate into that developed for axial loading τ_N in the case of pure axial loading, while each of them degenerate into that developed for bending about the corresponding principal axis (i.e $\tau_{MNy} \rightarrow \tau_{My}$ and $\tau_{MNz} \rightarrow \tau_{Mz}$) in the case of pure bending.

3.4. Moment gradient effect

Structural steel members typically experience varying bending moments along their lengths, which results in less extensive development of plasticity relative to members under uniform bending. Thus, the reduction to their flexural stiffnesses through the stiffness reduction functions developed for uniform bending in the previous subsections using the maximum bending moment values along the length would lead to overly-conservative designs. To consider the influence of moment gradient on the development of plasticity, two different approaches can be adopted: (i) multiplying the maximum bending moment values along the length by moment gradient factors C_m and using the resulting bending moments within the stiffness reduction functions τ_{MNy} and τ_{MNz} given by eq. (14) and eq. (15) respectively, whereby the flexural stiffnesses about the y and z axes are uniformly reduced along the length; this is referred to as the moment gradient approach [31, 32] or (ii) dividing the member into portions along its length and reducing the flexural stiffnesses of each portion on the basis of the bending moment values at the middle of each portion through τ_{MNy} and τ_{MNz}; this is referred to as the tapering approach [31, 32]. Owing to its more practical application, the former method, which is described in more detail in [31, 32], is utilised in this paper. The moment gradient factor C_m can be determined using the following equation:

$$C_m = \frac{-1.5M_{Ed,max} + 4M_A + 6M_B + 4M_C}{12.5M_{Ed,max}}, \tag{16}$$

where M_A, M_B and M_C are the absolute values of bending moments at the quarter, middle and three-quarter points along the length of the steel member and $M_{Ed,max}$ is the maximum absolute value of bending moment along the length. According to the proposed moment gradient approach, the maximum first-order bending moment about the principal y axis $M_{y,Ed,max}$ should be multiplied by the moment gradient factor C_m calculated considering the variation of the first-order bending moments about the y axis along the member length through eq. (16) (i.e. $M_{y,Ed} = C_m M_{y,Ed,max}$) and used in τ_{My} and τ_{MNy} as shown below:

$$\tau_{My} = 1.0 \quad \text{if} \quad C_m M_{y,Ed,max}/M_{y,pl} \leq \phi_y,$$

$$\tau_{My} = \tau_{Mly} + (1 - \tau_{Mly}) \left[1 - \left(\frac{\frac{C_m M_{y,Ed,max}}{M_{y,pl}} - \phi_y}{\xi_{my} - \phi_y} \right)^{\beta_{my}} \right]^{\frac{1}{\beta_{my}}} \quad \text{if} \quad \phi_y \leq \frac{C_m M_{y,Ed,max}}{M_{y,pl}} \leq \xi_{my},$$

$$\tau_{My} = \tau_{Mly} \left[1 - \left(\frac{\frac{C_m M_{y,Ed,max}}{M_{y,pl}} - \xi_{my}}{m_{ry} - \xi_{my}} \right) \right]^{1/\delta_{my}} \quad \text{if} \quad \xi_{my} \leq C_m M_{y,Ed,max}/M_{y,pl},$$

$$\tau_{MNy} = \tau_{My} \tau_N \left\{ 1 - \left(\frac{N_{Ed}}{N_{pl}} \right)^{\eta_y} \left(\frac{C_m M_{y,Ed,max}}{M_{y,pl}} \right)^{\rho_y} \right\}, \tag{17}$$

whereby the flexural stiffness of the member about the principal y axis (i.e. EI_y) is reduced at the same rate along the length. Similarly, the maximum first-order bending moment along the length about the principal z axis $M_{z,Ed,max}$ should be factored by C_m determined considering the variation of the first-order bending moments about the z axis along the length through eq. (16) (i.e. $M_{z,Ed} = C_m M_{z,Ed,max}$) and used in τ_{Mz} and τ_{MNz} as shown below:

$$\tau_{Mz} = 1.0 \quad \text{if} \quad C_m M_{z,Ed,max}/M_{z,pl} \leq \phi_y,$$

$$\tau_{Mz} = \tau_{Mlz} + (1 - \tau_{Mlz}) \left[1 - \left(\frac{\frac{C_m M_{z,Ed,max}}{M_{z,pl}} - \phi_z}{\xi_{mz} - \phi_z} \right)^{\beta_{mz}} \right]^{\frac{1}{\beta_{mz}}} \quad \text{if} \quad \phi_z \leq \frac{C_m M_{z,Ed,max}}{M_{z,pl}} \leq \xi_{mz},$$

$$\tau_{Mz} = \tau_{Mlz} \left[1 - \left(\frac{\frac{C_m M_{z,Ed,max}}{M_{z,pl}} - \xi_{mz}}{m_{rz} - \xi_{mz}} \right) \right]^{1/\delta_{mz}} \quad \text{if} \quad \xi_{mz} \leq C_m M_{z,Ed,max}/M_{z,pl},$$

$$\tau_{MNz} = \tau_{Mz} \tau_N \left\{ 1 - \left(\frac{N_{Ed}}{N_{pl}} \right)^{\eta_z} \left(\frac{C_m M_{z,Ed,max}}{M_{z,pl}} \right)^{\rho_z} \right\}, \tag{18}$$

whereby the flexural stiffness of the member about the principal z axis (i.e. EI_z) is reduced at the same rate along the length. Note that in the proposed moment gradient approach, the calculation of the values of the auxiliary coefficients for τ_{My} and τ_{Mz}, η_{yz} and η_{zy} should be carried out considering the maximum first-order bending moments along the member lengths.

3.5. Simplified stiffness reduction method

Although the implementation of the stiffness reduction scheme of the SRM developed in the previous subsection can readily be automated within structural analysis software or through simple spreadsheets, a simplified version, which will henceforth be referred to as the SRM – Simplified, is also proposed herein. The SRM – Simplified utilises the following stiffness reduction function for the reduction of flexural stiffness about the principal y axis:

$$\tau_{MNy,s} = \tau_N \left\{ 0.8 + 0.2 \left[\frac{1}{\pi/2} \arctan \left(\frac{N_{Ed}/N_{pl}}{M_{y,Ed,max}/M_{y,pl}} \right) \right]^{2.6} \right\}, \tag{19}$$

and the following stiffness reduction function for the reduction of flexural stiffness about the principal z axis:

$$\tau_{MNz,s} = \tau_N \left\{ 0.8 + 0.2 \left[\frac{1}{\pi/2} \arctan \left(\frac{N_{Ed}/N_{pl}}{M_{z,Ed,max}/M_{z,pl}} \right) \right]^{2.6} \right\}. \tag{20}$$

As can be seen from eq. (19) and eq. (20), the simplified stiffness reduction functions for the principal y and z axes, $\tau_{MNy,s}$ and $\tau_{MNz,s}$, utilise the stiffness reduction function developed for axial loading τ_N given by eq. (1), the maximum first-order bending moments along the member lengths about the principal y and z axes $M_{y,Ed,max}$ and $M_{z,Ed,max}$ and the axial load carried by the member N_{Ed}. Thus, the simplified functions degenerate into τ_N in the case of pure axial loading, while

they become equal to 0.8 in the case of pure bending, which approximately accounts for stiffness reduction due to bending.

In development of the simplified stiffness reduction functions $\tau_{MNy,s}$ and $\tau_{MNz,s}$, the stiffness reduction scheme adopted by the direct analysis method (DAM) of AISC 360-16 [2] was taken into consideration, which uses a constant stiffness reduction factor equal to 0.8 to approximately account for the influence of bending on the stiffness degradation of the structure in addition to the influence of the uncertainty with respect to the strength and stiffness of material. The DAM also utilises a stiffness reduction function derived using the Column Research Council (CRC) column buckling curve $\tau_{N,CRC}$ [33–35] to consider the adverse influence of plasticity resulting from axial loading N_{Ed} on structural behaviour, thereby adopting a stiffness reduction scheme equal to $\tau_{DAM} = 0.8\tau_{N,CRC}$ regardless of the value of the applied bending moments (i.e. $M_{y,Ed}$ and $M_{z,Ed}$). Since using a stiffness reduction function equal to $0.8\tau_N$ would lead to underpredictions of the ultimate strengths of steel members subjected primarily to axial compression, the expression in brackets within eq. (19) and eq. (20) was utilised in this study to obtain a transition from the stiffness reduction function for pure axial loading τ_N towards the lower bound value of the stiffness reduction function for combined axial loading and bending $0.8\tau_N$. Thus, the expression within the brackets is equal to 1.0 in the case of pure axial compression but transitions towards 0.8 with increasing applied bending, thereby enabling accurate estimations of the ultimate strengths of both columns and beam-columns by means of the SRM – Simplified. The exponent 2.6 within $\tau_{MNy,s}$ and $\tau_{MNz,s}$ was determined by calibrating the ultimate strength predictions obtained from the SRM – Simplified to those obtained from GMNIA considering hot-finished tubular beam-columns subjected predominantly to axial loading.

Comparison of the stiffness reduction functions for the SRM τ_{MNy} given by eq. (14) and for the SRM – Simplified $\tau_{MNy,s}$ given by eq. (19) for a beam-column with an SHS 100×5 profile and subjected to monoaxial bending $M_{y,Ed}$ plus axial compression N_{Ed} is shown in Fig. 6. Note that $\tau_{MNy} = \tau_{MNz}$ and $\tau_{MNy,s} = \tau_{MNz,s}$ for SHS regardless of the axis of the applied bending. As can be seen from the figure, τ_{MNy} and $\tau_{MNy,s}$ are equal when a member is subjected to pure axial loading (i.e. $N_{Ed} > 0$, $M_{y,Ed} = 0$). As the applied bending increases, $\tau_{MNy,s}$ reduces more rapidly relative to τ_{MNy} in the region where the applied axial loading is small (i.e. $N_{Ed}/N_{pl} < 0.2$), whereas the rate of reduction of $\tau_{MNy,s}$ is more gradual when the applied axial loading is such that $N_{Ed}/N_{pl} \geq 0.2$. Fig. 6 also shows that τ_{MNy} approaches zero when the applied bending moment $M_{y,Ed}$ approaches the plastic bending moment resistance $M_{y,pl}$ (i.e. $M_{y,Ed} \geq 0.95M_{y,pl}$), whereas $\tau_{MNy,s}$ assumes a lower bound value equal to $0.8\tau_N$ regardless of the applied bending moment value $M_{y,Ed}$. However, this does not lead to unsafe results for the SRM – Simplified as tubular structural elements are not sensitive to instability effects in the cases where $M_{y,Ed} \geq 0.95M_{y,pl}$ since the applied axial loading has to assume very small values so that the ultimate cross-section strength of the member is not exceeded. Finally, some regions of the stiffness reduction functions shown in Fig. 6 corresponding to very low values applied axial loading $N_{Ed} < 0.1N_{pl}$ with very low values of applied bending $M_{y,Ed} < 0.1M_{y,pl}$ or those corresponding to the applied axial loading and bending moments exceeding the ultimate cross-section strengths are not of practical significance.

It should be noted that in addition to being very practical, another advantage of the SRM – Simplified is that its stiffness reduction functions depend only on the applied axial force level and are independent of the applied bending moments. Thus, when the SRM – Simplified is applied

to a structure, changes of member sizes during the design do not affect the originally determined stiffness reduction factors since the internal axial force distribution is insensitive to changes of member sizes. This advantage of making stiffness reduction functions independent of applied bending moments has also been pointed out by Surovek-Maleck and White [12].

Though the stiffness reduction scheme of the SRM - Simplified is already quite simple, a further simplification of the method is also investigated in this paper, where the flexural stiffnesses of the investigated tubular members about their principal axes were reduced by $0.8\tau_N$ (i.e. $\tau_{MNy,s} = \tau_{MNz,s} = 0.8\tau_N$) similar to the direct analysis method of [2]. This approach is referred to as the SRM - Simplified $0.8\tau_N$ in this paper. Both the SRM - Simplified and SRM - Simplified $0.8\tau_N$ are compared against the SRM in this paper, which uses the more advanced stiffness reduction functions.

3.6. Ultimate cross-section strength equations

Owing to their simplicity, the continuous ultimate cross-section strength equations recommended by Duan and Chen [30] are adopted in this study, which have the general format provided below for all types of cross-section:

$$1/\alpha_{ult,c} = \left[\frac{M_{y,Ed}/M_{y,pl}}{1-\left(N_{Ed}/N_{pl}\right)^{\beta_{cy}}}\right]^{\alpha_{cy}} + \left[\frac{M_{z,Ed}/M_{z,pl}}{1-\left(N_{Ed}/N_{pl}\right)^{\beta_{cz}}}\right]^{\alpha_{cz}} \leq 1.0. \tag{21}$$

where $1/\alpha_{ult,c}$ is the utilisation ratio of the cross-section. In Duan and Chen [30], the values of $\alpha_{cy}, \alpha_{cz}, \beta_{cy}, \beta_{cz}$ were recommended to be taken as $\alpha_{cy} = \alpha_{cz} = 2.0$ and $\beta_{cy} = \beta_{cy} = 1.75$ for CHS and $\alpha_{cy} = \alpha_{cz} = 1.7 + 1.5N_{Ed}/N_{pl}$ and $\beta_{cy} = 2 - 0.5(b/h) \geq 1.3$ and $\beta_{cz} = 2 - 0.5(h/b) \geq 1.3$ for SHS and RHS. During the calibration of the stiffness reduction functions τ_{MNy} and τ_{MNz}, it was observed that the use of these values with eq. (21) to make cross-section strength checks for CHS, SHS and RHS led to overpredictions of stiffness reduction for members with intermediate-to-high slenderness values. Moreover, as observed by Kucukler [36] and Kucukler et al. [22], when reduced stiffness is applied to a structure from the outset of the analysis, rather than gradually under increasing loading, the overprediction of stiffness reduction for members with intermediate-to-high slenderness leads to (i) a structural response that is considerably more flexible than that achieved through GMNIA, resulting in overestimations of drifts and second-order $P-\Delta$ moments and (ii) underpredictions of bending moments distributed from beams to columns as the latter typically experience higher degrees of stiffness reduction. Thus, for the purpose of achieving accurate and safe strength predictions for members over the full slenderness range and avoiding the overestimations of the actual levels of stiffness degradation in steel structures, the values of $\alpha_{cy}, \alpha_{cz}, \beta_{cy}, \beta_{cz}$ recommended by [30] are slightly modified herein, leading to more conservative ultimate cross-strength estimations. For SHS and RHS, the lower bound values recommended by Duan and Chen [30] $\beta_{cy} = \beta_{cz} = 1.3$ were adopted. For CHS, it was also decided to use $\beta_{cy} = \beta_{cz} = 1.3$; this value is compatible with the β_{cy} and β_{cz} values for SHS and RHS and the β_{cy} value recommended for I-sections in [21, 22]. For SHS and RHS, α_{cy} and α_{cz} were taken as $\alpha_{cy} = \alpha_{cz} = 1.4$, while for CHS α_{cy} and α_{cz} were taken as $\alpha_{cy} = \alpha_{cz} = 2$, considering GMNIA results for beam-columns subjected to biaxial bending plus axial compression. Thus, the recommended

ultimate cross-section strength equation for CHS is given by the expression below:

$$1/\alpha_{ult,c} = \left[\frac{M_{y,Ed}/M_{y,pl}}{1-\left(N_{Ed}/N_{pl}\right)^{1.3}}\right]^{2} + \left[\frac{M_{z,Ed}/M_{z,pl}}{1-\left(N_{Ed}/N_{pl}\right)^{1.3}}\right]^{2} \leq 1.0. \tag{22}$$

and the recommended ultimate cross-section strength equation for SHS and RHS is as follows:

$$1/\alpha_{ult,c} = \left[\frac{M_{y,Ed}/M_{y,pl}}{1-\left(N_{Ed}/N_{pl}\right)^{1.3}}\right]^{1.4} + \left[\frac{M_{z,Ed}/M_{z,pl}}{1-\left(N_{Ed}/N_{pl}\right)^{1.3}}\right]^{1.4} \leq 1.0. \tag{23}$$

It should be noted that to preclude overpredictions of the actual levels of stiffness degradation experienced by steel structures, the direct analysis method of AISC 360-16 [2], which is also applied by reducing the stiffness of the members of a structure from the onset of the structural analysis, also uses a single and conservative ultimate cross-section strength equation for all cross-section shapes, leading to underpredictions of ultimate cross-section strengths for tubular cross-sections and I-sections under minor axis bending plus compression. However, these underpredictions only arise for stocky members for which the ultimate resistance is primarily governed by cross-section failure. Moreover, stocky members with Class 1 sections typically experience strain hardening, attaining ultimate cross-section resistances greater than the plastic cross-section strengths. For the case of members with intermediate-to-high slenderness subjected to instability effects, which constitute the majority of steel members in structures, both the SRM and direct analysis methods lead to more accurate strength predictions relative to stocky members for which both methods lead to satisfactorily accurate and safe ultimate strength predictions.

3.7. Implementation of the proposed stiffness reduction method

The implementation of the proposed stiffness reduction method involves the following steps:

(i) Determine stiffness reduction factors for the principal y and z axes (i.e. τ_{MNy} and τ_{MNz} or $\tau_{MNy,s}$ and $\tau_{MNz,s}$) through eq. (14) and eq. (15) or eq. (19) and eq. (20), using the first-order axial loads and bending moments carried by the member.

(ii) Reduce the flexural stiffnesses of the tubular member about the principal y and z axes (i.e. EI_y and EI_z) using the corresponding stiffness reduction factors.

(iii) Perform Linear Buckling Analysis of the member with reduced stiffnesses (LBA-SR) and ensure that the lowest buckling load amplifier $\alpha_{cr,i}$ is greater than or equal to 1.0 (i.e. $\alpha_{cr,i} \geq 1.0$).

(iv) Perform Geometrically Nonlinear Analysis of the member with reduced stiffnesses (GNA-SR), perform cross-section strength checks using eq. (22) or eq. (23) and ensure that the cross-section strength is not exceeded along the length (i.e. $1/\alpha_{ult,c} \leq 1.0$).

The proposed stiffness reduction method should be applied using structural analysis software able to consider fully both $P-\delta$ and $P-\Delta$ effects. It should also be noted that for application of all the three stiffness reduction methods (SRM, SRM – Simplified and SRM - Simplified $0.8\tau_N$), the reduction of flexural stiffnesses of the members about the principal axes (i.e. EI_y and EI_z) should be achieved by reducing the second moment areas about these axes (i.e. I_y and I_z) through the corresponding stiffness reduction function for each principal axis.

Finally, it should be noted that the proposed approach is currently applicable to hot-finished tubular steel members with (i) Class 1 and 2 sections and (ii) not susceptible to lateral-torsional buckling; the latter condition can be ensured by assessing whether the non-dimensional lateral-torsional buckling slenderness $\overline{\lambda}_{LT}$ of a tubular member, determined by taking the square root of the ratios between the plastic bending moment resistance $M_{pl,Rd}$ and the elastic critical buckling moment M_{cr}, is smaller than or equal to 0.2 (i.e. $\overline{\lambda}_{LT} = \sqrt{M_{pl,Rd}/M_{cr}} \leq 0.2$). Additionally, the proposed stiffness reduction methods are limited to hot-finished tubular steel members with maximum applied shear forces $V_{Ed,max}$ less than the half of the cross-sectional shear resistance $V_{pl,Rd}$ (i.e. $V_{Ed,max} \leq 0.5V_{pl,Rd}$). The proposed SRM are also only applicable in the cases where the cross-sections are not susceptible to shear buckling, which can be checked using the relevant provisions given in EN 1993-1-5 [37].

4. Stiffness reduction method for the design of beam-columns under axial compression and monoaxial bending

The proposed SRM is applied to a series of simply-supported beam-columns subjected to axial compression plus monoaxial bending in this section considering various CHS and SHS/RHS types, slenderness values and loading conditions. The higher accuracy of the proposed approach for members with rotational restraints at the ends relative to traditional design is also illustrated.

4.1. Tubular beam-columns subjected to axial compression plus uniform monoaxial bending

A comparison of the ultimate strength predictions obtained through the SRM, SRM – Simplified and SRM – Simplified $0.8\tau_N$ against those determined through GMNIA is illustrated in Fig. 7 for laterally restrained beam-columns with CHS 244.5 × 5.6, SHS 100 × 100 × 5 and RHS 300 × 100 × 16 sections subjected to axial compression plus monoaxial bending. In the case of the RHS 300 × 100 × 16 beam-columns, the accuracy of the method was assessed for both major and minor axis bending plus axial compression. Three non-dimensional slenderness values for flexural buckling about the major and minor axes, $\overline{\lambda}_y$ and $\overline{\lambda}_z$, equal to 0.4, 1.0 and 1.5, determined by taking the square root of the ratios between the axial yield load N_{pl} and elastic critical loads about the major and minor axes, $N_{cr,y}$ and $N_{cr,z}$, (i.e. $\overline{\lambda}_y = \sqrt{N_{pl}/N_{cr,y}}$ and $\overline{\lambda}_z = \sqrt{N_{pl}/N_{cr,z}}$), were considered, thus assessing the accuracy of the proposed approaches for beam-columns with low, moderate and high slenderness. As can be seen from Fig. 7, the proposed SRM, SRM – Simplified and SRM – Simplified $0.8\tau_N$ lead to accurate ultimate strength predictions (i.e. close to the results from GMNIA) for all different section types, slenderness values and ratios between axial loading and bending moments, though the SRM – Simplified $0.8\tau_N$ underpredicts the ultimate strengths in the cases where the axial loading is dominant.

The SRM, SRM – Simplified and SRM – Simplified $0.8\tau_N$ are also compared against the beam-column design methods provided in the Annex A and Annex B of EN 1993-1-1 [1] in Fig. 7. As can be seen from the figure, the proposed SRM and SRM – Simplified both lead to the same high level of accuracy as that achieved through these methods for laterally restrained beam-columns under constant bending plus axial compression.

In addition to the beam-columns illustrated in Fig. 7, the accuracy of the proposed approaches was also assessed for 630 laterally restrained beam-columns subjected to uniform monoaxial bending about the major and minor axes with non-dimensional slendernesses $\overline{\lambda}_y = 0.4, 1.0, 1.5$ and $\overline{\lambda}_z = 0.4, 1.0, 1.5$, and with 7 CHS and 7 SHS/RHS section types. The range of the geometrical properties of the considered cross-sections is provided in Table 1. The accuracy of the proposed approaches is assessed through the ϵ parameter calculated using the following equation:

$$\epsilon = \frac{R_{SRM}}{R_{GMNIA}} = \frac{\sqrt{\left(N_{Ed,max,SRM}/N_{pl}\right)^2 + \left(M_{Ed,max,SRM}/M_{pl}\right)^2}}{\sqrt{\left(N_{Ed,max,GMNIA}/N_{pl}\right)^2 + \left(M_{Ed,max,GMNIA}/M_{pl}\right)^2}}, \tag{24}$$

where R_{SRM} and R_{GMNIA} are the radial distances from the origin to the ultimate strength $N_{Ed} - M_{Ed}$ interaction curves determined through the stiffness reduction approaches and GMNIA respectively, $N_{Ed,SRM,max}$ and $N_{Ed,GMNIA,max}$ are the ultimate axial load strengths determined through the stiffness reduction approaches and GMNIA, $M_{Ed,SRM,max}$ and $M_{Ed,GMNIA,max}$ are the ultimate bending moment strengths obtained from the stiffness reduction approaches and GMNIA respectively and β_R is the angle of the radial distances, as illustrated in Fig. 8. Thus, ϵ values larger than 1.0 indicate overpredictions of the ultimate strength by the proposed approaches. In Table 7, ϵ_{av}, ϵ_{COV}, ϵ_{max} and ϵ_{min} represents the average, coefficient of variation, maximum and minimum values of ϵ. Note that ten different angles β_R ranging between 11.25° and 90° in increments of 11.25° were considered within the interaction curves for each cross-section type and slenderness value. As can be seen from Table 5, the proposed SRM, SRM – Simplified and SRM – Simplified $0.8\tau_N$ all lead to accurate and safe ultimate strength predictions for the considered wide range of slendernesses and section types. Table 5 also shows that the accuracy of the proposed SRM decreases with the simplification of the stiffness reduction functions.

The accuracy of the beam-column design methods provided in the Annex A and Annex B of EN 1993-1-1 [1] is also assessed against the proposed stiffness reduction approaches in Table 5 for all the considered 630 beam-columns, where ϵ values are determined by taking the ratios of the radial distances to the interaction curves obtained from these methods to those determined through GMNIA. Table 5 shows that the beam-column design methods of Eurocode 3 also lead to very accurate ultimate strength predictions, though their accuracy is slightly lower relative to the SRM and SRM – Simplified.

4.2. Tubular beam-columns subjected to axial compression plus varying monoaxial bending along the lengths

In this subsection, the accuracy of the proposed stiffness reduction approaches is assessed for simply-supported laterally restrained beam-columns under axial compression plus varying bending along their lengths. Different values for the ratios between the end moments, leading to single-

and double-curvature bending, are taken into account. Comparisons of the ultimate strength predictions obtained from the SRM, SRM – Simplified and SRM – Simplified $0.8\tau_N$ against those determined through GMNIA are illustrated in Fig. 9 for beam columns with CHS 244.5×5.6, SHS 100×100 and RHS $300 \times 100 \times 16$ sections and non-dimensional slenderness $\overline{\lambda}_y = 0.4, 1.0, 1.5$ and $\overline{\lambda}_z = 0.4, 1.0, 1.5$, subjected to axial compression and end-moments with different ratios μ. Note that $M_{y,Ed}$ and $M_{z,Ed}$ are limited to the plastic bending moment resistances $M_{y,pl}$ and $M_{z,pl}$ in the figure, although these values were exceeded in the GMNIA of some beam-columns due to strain hardening. As can be seen from Fig. 9, the proposed stiffness reduction approaches lead to accurate strength predictions for both single- and double-curvature bending, different slenderness values, section shapes, as well as both major and minor axis bending for the beam-columns with rectangular cross-sections. The SRM is generally more accurate relative to the SRM – Simplified owing to its more advanced stiffness reduction functions, while the SRM – Simplified $0.8\tau_N$ leads to underpredictions of the strengths when the axial loading is dominant similar to the observations made for the beam-columns under uniform bending plus axial compression. It should also be noted that in Fig. 9, the ultimate strengths obtained from GMNIA for members (particularly for beam-columns with $\overline{\lambda}_z = 0.4$) subjected to low axial loads exceed the ultimate plastic cross-section resistances due to the occurrence of strain hardening. Since strain hardening is neglected in the proposed SRM similar to the beam-column design methods provided in EN 1993-1-1 [1] and AISC 360-16 [2], the ultimate resistances of these beam-columns are underpredicted. Also, the maximum moments are limited to $M_{y,pl}$ in Fig. 9. The accuracy of the SRM was also assessed against the beam-column design methods provided in Annex A and Annex B of Eurocode 3 [1] in Fig. 9. As can be seen from the figure, both methods lead to accurate strength predictions, though the proposed stiffness reduction approaches lead to more accurate results particularly for beam-columns under full double-curvature bending with $\mu = -1$.

The proposed stiffness reduction approaches were also assessed against GMNIA results on for 1824 laterally-restrained beam-columns subjected to axial compression plus varying monoaxial bending along their lengths. Four different end moment ratios (i.e. $\mu = 0.5, 0, -0.5, -1$) were considered, where the beam-columns were subjected to single- and double curvature bending. The accuracy of the proposed stiffness reduction approaches for beam-columns subjected to different end-moment ratios are provided in Table 6 for CHS beam-columns, in Table 7 for RHS beam-columns subjected to major axis bending and in Table 8 for RHS beam-columns subjected to minor axis bending. For the investigated beam-columns, 7 CHS and 7 RHS were considered whose range of geometrical properties are provided in Table 1. Note that ϵ values were determined as described in the previous subsection, considering 10 different radial angles β_R varying between 11.25° and 90° in an increment of 11.25° for each cross-section shape, slenderness and loading condition. The cases where the ultimate strengths of beam-columns obtained from GMNIA exceeded the ultimate plastic cross-section strengths due to strain hardening were not included in Tables 6, 7 and 8. As can be seen from Tables 6, 7 and 8, the SRM and the SRM – Simplified lead to very accurate strength predictions for all the laterally restrained tubular columns with different cross-section shapes, slendernesses and end-moment ratios, though note that the SRM is more accurate than the SRM – Simplified for all the considered cases. The accuracy of the SRM – Simplified $0.8\tau_N$ is lower, but it still remains reasonable as can be seen from the tables. The proposed stiffness

reduction approaches are also compared against the Eurocode 3 [1] Annex A and Annex B design methods in Tables 6, 7 and 8, where it is seen that the SRM generally leads to a higher level of accuracy relative to these methods, while the SRM – Simplified generally leads to a similar level of accuracy achieved through the beam-column design methods of Eurocode 3 [1].

4.3. Tubular beam-columns with elastic rotational restraints

The proposed stiffness reduction approaches are applied to a series of laterally restrained tubular beam-columns with elastic rotational restraints at the both ends and subjected to axial compression plus uniformly distributed loading in this subsection. The considered case represents a steel column within a non-sway steel frame, supported rotationally at both ends by the neighbouring steel beams and columns. The same spring stiffnesses were utilised for both rotational springs at the ends of the beam-columns, which had an RHS 200 × 100 × 10 cross-section. The ultimate strength predictions obtained through the SRM, SRM – Simplified and SRM – Simplified $0.8\tau_N$ are compared against those obtained from GMNIA for beam-columns with rotational spring stiffnesses of $K_\theta = 4EI_y/L$ and $K_\theta = EI_y/L$ in Fig. 10 (a) and (b) respectively, where L is the length of the member and I_y is the second moment of area of its cross-section about the major (y-y) axis. Three non-dimensional slendernesses calculated considering the flexural buckling loads of the columns without end restraints (i.e. $\overline{\lambda}_{y,0} = \sqrt{N_{pl}/(\pi^2 EI_y/L^2)}$ equal to 0.4, 1.0 and 1.5 were considered. Fig. 10 shows that the SRM and SRM – Simplified lead to very accurate ultimate strength predictions for the beam-columns with elastic rotational restraints at the ends. The SRM – Simplified $0.8\tau_N$ is also accurate but somewhat underestimates the strengths of beam-columns subjected to predominantly axial compression. The support afforded by the elastic rotational springs increases with the development of plasticity within the beam-columns, which is accurately accounted for by the proposed stiffness reduction approaches, as can be seen from Fig. 10. The strength predictions estimated using the Eurocode 3 [1] Annex A and Annex B design methods are also compared against those obtained from GMNIA in Fig. 10. In the application of the Eurocode 3 beam-column design methods, the non-sway buckling lengths calculated for the considered rotational spring values were utilised and the moment gradient factors used in these methods were back-calculated by performing Geometrically Nonlinear Analyses of the beam-columns in accordance with the recommendations of [11, 38], highlighting the need for additional calculation effort in the Eurocode 3 design methods for beam-columns that are not simply-supported, unlike the proposed stiffness reduction approaches. As can be seen from Fig. 10, the proposed stiffness reduction approaches generally lead to a significantly higher level of accuracy in comparison to the Eurocode 3 [1] Annex A and Annex B beam-column design methods, which can be ascribed both to the neglect of the increased effectiveness of the rotational springs with the development of plasticity within the beam-columns and their decreased level of accuracy for beam-columns that do not have simply-supported end conditions, as also indicated by [11]. Fig. 10 also shows that similar to that observed for beam-columns under moment gradients, the occurrence of strain hardening leads to strengths of beam-columns with $\overline{\lambda}_z = 0.4$ exceeding the ultimate plastic cross-section resistances, where the SRM underpredicts the strengths of these members due to its neglect of strain hardening. Also in Fig. 10, the maximum moments are limited to $M_{y,pl}$ similar to Fig. 9.

4.4. Laterally unrestrained tubular beam-columns under axial compression plus monoaxial bending

The proposed stiffness reduction approaches are applied to laterally unrestrained beam-columns with an RHS 300 × 100 × 16 cross-section subjected to axial compression plus uniform major-axis bending with $\overline{\lambda}_z$ equal to 0.4, 1.0 and 1.5 in this subsection. The ultimate strength predictions of the beam-columns determined through the proposed stiffness reduction approaches are compared against those obtained from GMNIA in Fig. 11 (a). As can be seen from the figure, the proposed SRM and SRM – Simplified approaches lead to rather significant overestimations of the ultimate strengths for some beam-columns with non-dimensional slenderness $\overline{\lambda}_z$ of 1.0 and 1.5, which buckle inelastically about their minor axis after experiencing significant pre-buckling deformations in the in-plane (i.e. in the plane of bending) direction. The pre-buckling deformations result in an increased level of plasticity with the development of significant second-order in-plane (i.e. major axis) bending moments within the members. Since these in-plane pre-buckling deformations and their influence on the development of an increased level of plasticity are neglected by the SRM and SRM – Simplified, they lead to unconservative results for these beam-columns. Note that the pre-buckling in-plane deformations are also disregarded in the SRM – Simplified $0.8\tau_N$, but the rather conservative stiffness reductions now lead to improved predictions of ultimate strengths. To consider the detrimental influence of the pre-buckling deformations prior to the out-of-plane failure, the following additional steps are recommended after step (iv) described in the subsection 3.7 for beam-columns with rectangular cross-sections:

(v) Reduce the minor axis flexural stiffness of the member (i.e. EI_z) through the stiffness reduction function for axial loading $\tau_{Nz,r}$, using the reduced axial force resistance $N_{pl,r}$ due to the development of in-plane second-order bending moments from GNA-SR.

(vi) Implement Linear Buckling Analysis of the member with this reduced stiffness and ensure that lowest buckling load amplifier $\alpha_{cr,i}$ is greater than or equal to 1.0 (i.e. $\alpha_{cr,i} \geq 1.0$).

The reduced axial force resistance $N_{pl,r}$ is determined considering second-order major axis bending moments obtained from Geometrically Nonlinear Analysis with stiffness reduction (GNA-SR) of the member after the step (iv) described in the subsection 3.7 and using the following equation:

$$N_{pl,r} = N_{pl}\left(1 - \frac{M_{y,Ed,GNA-SR,max}}{M_{y,pl}}\right)^{1/1.3}, \tag{25}$$

where $M_{y,Ed,GNA-SR,max}$ is the maximum second-order major axis bending moment along the length obtained from the GNA-SR of the member. Utilising the reduced axial force resistance $N_{pl,r}$, the stiffness reduction function for the flexural buckling about the minor axis considering pre-buckling deformations $\tau_{Nz,r}$ is determined using the following expression:

$$\tau_{Nz,R} = \frac{4\psi^2}{\alpha^2 N_{Ed}/N_{pl,r}\left[1 + \sqrt{1 - 4\psi\frac{N_{Ed}/N_{pl,r} - 1}{\alpha^2 N_{Ed}/N_{pl,r}}}\right]^2} \quad \text{but} \quad \tau_{Nz,R} \leq 1$$

$$\text{where} \quad \psi = 1 + 0.2\alpha\frac{N_{Ed}}{N_{pl,r}} - \frac{N_{Ed}}{N_{pl,r}}. \tag{26}$$

Note that the additional steps (v) and (vi) are recommended only in the implementation of the SRM and SRM – Simplified since the SRM – Simplified $0.8\tau_N$ does not provide significant over-predictions of the ultimate strengths as can be seen from Fig. 11 (a). Moreover, the additional steps (v) and (vi) should also be applied in the implementation of the SRM and SRM – Simplified to RHS beam-columns under biaxial bending moments and axial compression, which are investigated in the following section, as it may control the design in the cases where the applied major axis bending is dominant relative to the applied minor axis bending.

The ultimate strength predictions obtained through the SRM and SRM – Simplified considering the influence of the pre-buckling deformations are compared against those obtained from GMNIA in Fig. 11 (b), showing that the proposed way of considering the influence of the pre-buckling deformations in the SRM and SRM – Simplified leads to safe and very accurate ultimate strength predictions. The ultimate strengths determined through the Eurocode 3 [1] Annex A and Annex B beam-column design methods are also provided in Fig. 11 (a). Comparing Fig. 11 (a) and (b), it can be seen that the proposed SRM and SRM – Simplified generally lead to a higher level of accuracy relative to the Eurocode 3 [1] beam-column design methods.

5. Stiffness reduction method for the design of beam-columns under axial compression plus biaxial bending

The proposed stiffness reduction approaches are applied to a series of tubular beam-columns subjected to axial compression plus biaxial bending in this section. Comparisons of the ultimate strengths obtained from the stiffness reduction approaches and GMNIA for beam-columns with an RHS $200 \times 100 \times 10$ cross-section under axial compression plus uniform major axis and minor axis bending are shown in Fig. 12. Three non-dimensional slenderness for flexural buckling about the minor axis $\overline{\lambda}_z$ equal to 0.4, 1.0 and 1.5 were considered; the beam-columns with $\overline{\lambda}_z = 0.4$ and $\overline{\lambda}_z = 1.0$ were subjected to axial load ratios $n = N_{Ed}/N_{pl} = 0.2, 0.4, 0.6$, while the beam-columns with $\overline{\lambda}_z = 1.5$ were subjected to axial load ratios $n = N_{Ed}/N_{pl} = 0.1, 0.2, 0.3$. Note that in the GMNIA, the axial compression was applied first, and then biaxial bending was applied simultaneously about the principal axes while the applied axial load was kept constant. Fig. 12 shows that the proposed SRM, SRM – Simplified and SRM – Simplified $0.8\tau_N$ all lead to accurate and safe-sided ultimate strength predictions for tubular beam-columns under axial compression plus uniform biaxial bending. As can be seen in Fig. 12 (a), the proposed stiffness reduction methods provide rather conservative ultimate strength predictions for members with $\overline{\lambda}_z = 0.4$. This results from the adoption of the modified conservative ultimate cross-section strength equation provided in eq. (23), which was necessary to prevent overestimation of the actual stiffness degradation of steel members, which may lead to a structural response that is considerably more flexible than that achieved through GMNIA and underestimations of bending moments distributed from beams to columns. It is worth noting that these underestimations significantly reduce for members with $\overline{\lambda}_z \geq 0.4$. The ultimate strengths estimated through the Eurocode 3 [1] Annex A and Annex B design methods are also provided in Fig. 12, illustrating that the proposed stiffness reduction approaches generally lead to a higher level of accuracy in comparison to the Eurocode 3 [1] beam-column design methods.

The SRM, SRM – Simplified and SRM – Simplified $0.8\tau_N$ are also assessed for beam-columns with a CHS 114.3×3.6 cross-section and non-dimensional slendernesses $\overline{\lambda}_z$ of 0.4, 1.0 and 1.5 in Fig. 13. Fig. 13 shows that applying the stiffness reduction to the flexural stiffnesses associated with the axes about which the bending moments are applied, the proposed SRM, SRM – Simplified and SRM – Simplified lead to accurate ultimate strength predictions for beam-columns with different slendernesses and axial compression values. It should be noted that in the application of the SRM to individual CHS beam-columns, the use of the combination of the bending moments applied about the two axes $M_{Ed} = \sqrt{M_{y,Ed}^2 + M_{z,Ed}^2}$ and assuming that the member is subjected to this monoaxial bending moment is recommended. The reduction of flexural stiffnesses of CHS members about the orthogonal axes is recommended in the application of the proposed stiffness reduction approaches to space frames involving CHS members, which will be thoroughly investigated in a future study.

The accuracy of the proposed stiffness reduction approaches was also investigated for 906 simply-supported beam-columns with an RHS $200 \times 100 \times 5$ cross-section and non-dimensional slenderness $\overline{\lambda}_z$ of 0.4, 1.0 and 1.5, subjected to axial compression plus biaxial bending, in Table 9. Note that for beam-columns with non-dimensional slenderness $\overline{\lambda}_z$ of 0.4 and 1.0, axial compressive load levels $n = N_{Ed}/N_{pl} = 0.2, 0.4$ and 0.6 were considered, while for those with $\overline{\lambda}_z = 1.5$, axial compressive load levels $n = N_{Ed}/N_{pl} = 0.2, 0.4$ and 0.6 were used. In all cases, the axial loads were applied first and then the bending moments were applied while the axial loads were kept constant. The ϵ values, describing the radial errors, were determined using the following expression:

$$\epsilon = \frac{R_{SRM}}{R_{GMNIA}} = \frac{\sqrt{\left(N_{Ed}/N_{pl}\right)^2 + \left(M_{y,Ed,SRM,max}/M_{y,pl}\right)^2 + \left(M_{z,Ed,SRM,max}/M_{z,pl}\right)^2}}{\sqrt{\left(N_{Ed}/N_{pl}\right)^2 + \left(M_{y,Ed,GMNIA,max}/M_{y,pl}\right)^2 + \left(M_{z,Ed,GMNIA,max}/M_{z,pl}\right)^2}}, \tag{27}$$

where R_{SRM} and R_{GMNIA} are the radial distances to the ultimate strength $N_{Ed} - M_{y,Ed} - M_{z,Ed}$ interaction curves determined through the proposed stiffness reduction approaches and GMNIA, $M_{y,Ed,SRM,max}$ and $M_{z,Ed,SRM,max}$ are the ultimate major and minor axis bending strengths determined through the proposed stiffness reduction approaches, while $M_{y,Ed,GMNIA,max}$ and $M_{z,Ed,GMNIA,max}$ are the ultimate major and minor axis bending strengths obtained from GMNIA respectively. In Table 9, the cases where the ultimate strengths of the beam-columns obtained from GMNIA exceeded the ultimate cross-section strengths due to strain hardening are not included and six different radial angles β_R ranging between 0° and 90° in increments of 18° were considered for each loading condition, slenderness and axial compression value. As can be seen from Table 9, various different combinations of major and minor axis end-moments were considered, leading to 25 different loading conditions for the considered beam-columns. The accuracy of the SRM and SRM – Simplified was assessed for the cases where the pre-buckling deformations were considered by means of the step (v) described in the subsection 4.4 and for those where they were disregarded. Table 9 shows that the proposed SRM and SRM – Simplified lead to very accurate and safe-sided ultimate strength predictions when the pre-buckling deformations are taken into account; the SRM provides a higher level of accuracy relative to the SRM – Simplified owing to its more advanced stiffness reduction functions. The SRM and SRM – Simplified are also accurate when the pre-buckling deformations are neglected, though there exist some significant overestimations for some

beam-columns (i.e. ϵ_{max} = 1.10). It should however be noted that only 6-7% of the ϵ values were larger than 1.05 when the pre-buckling deformations were neglected in the implementation of the SRM and SRM – Simplified. The level of accuracy achieved through the SRM – Simplified $0.8\tau_N$ is lower relative to the SRM and SRM – Simplified, but it is still satisfactory, showing that even the simple application of the stiffness reduction approach can lead to reasonably accurate ultimate strength predictions.

The proposed stiffness reduction approaches are also compared against the Eurocode 3 [1] Annex A and Annex B design methods in Table 9 for 906 beam-columns, for which ϵ values were determined considering the radial distances to the ultimate strength interaction curves obtained from these design methods and those determined through GMNIA. As can be seen from the table, the SRM, SRM – Simplified and SRM – Simplified $0.8\tau_N$ all lead to a higher level of accuracy in comparison to the Eurocode 3 [1] beam-column design methods for all the wide range of considered loading conditions and slendernesses.

6. Conclusions

In this paper, a stiffness reduction method (SRM) for the design of tubular steel members is developed. Stiffness reduction functions that fully capture the adverse influence of the plasticity and imperfections on member strengths were derived. Finite element models of tubular members were created, whose Geometrically and Materially Nonlinear Analyses with Imperfections (GMNIA) furnished benchmark data used for the verification of the SRM. The proposed SRM is implemented by first reducing the flexural stiffness of a member through the developed stiffness reduction functions and then performing an elastic Linear Buckling Analysis (LBA) and Geometrically Nonlinear Analysis (GNA) of the member. The developed stiffness reduction functions are able to consider the influence of combined axial loading and biaxial bending, thus making the proposed SRM applicable in this most general loading condition unlike that of [21]. Simplified versions of the proposed SRM using less advanced stiffness reduction functions but still able to consider fully the adverse effects of imperfections and plasticity were also proposed, which were referred to as the SRM – Simplified and SRM – Simplified $0.8\tau_N$, providing a very practical way of designing tubular members.

The proposed SRM, SRM – Simplified and SRM – Simplified $0.8\tau_N$ were verified for 630 laterally restrained tubular beam-columns subjected to axial compression plus uniform monoaxial bending and for 1824 laterally restrained tubular beam-columns under axial compression plus moment gradients, considering various CHS and RHS profiles, slendernesses and moment gradients including both single- and double-curvature bending. The proposed approaches were also compared against the Eurocode 3 [1] Annex A and Annex B beam-column design methods for these cases. The results showed that proposed SRM generally leads to a higher level of accuracy in comparison to these methods, while the accuracy level of the SRM – Simplified was similar and that of the SRM – Simplified $0.8\tau_N$ was slightly lower, albeit still satisfactory. The proposed stiffness reduction approaches were also applied to tubular beam-columns with elastic rotational restraints at the ends, for which it was observed that they provide significantly more accurate ultimate strength predictions relative to the Eurocode 3 [1] beam-column design methods owing to their consideration of the increased effective support afforded by the rotational end restraints with

the development of plasticity within the beam-columns. Overpredictions of ultimate strength were observed for the SRM and SRM – Simplified when applied to laterally unrestrained RHS beam-columns under axial compression plus major axis bending failing about the minor axis when the pre-buckling effects were neglected. To eliminate these unconservative results, additional steps are recommended in the implementation of the SRM and SRM – Simplified for RHS beam-columns to consider the detrimental pre-buckling effects, which then provided safe-sided and accurate results. Finally, the proposed stiffness reduction approaches were verified for 906 simply-supported tubular beam-columns under axial compression plus biaxial bending considering different slendernesses, axial compression values and 25 different loading conditions. It was observed that the proposed stiffness reduction approaches lead to very accurate and safe-sided ultimate strength predictions for the wide range of considered cases and their accuracy is generally higher relative to the beam-column design methods of Eurocode 3 [1].

The developed stiffness reduction approaches can readily be applied through any conventional structural analysis software and remove the need to use member design equations or model out-of-straightnesses, only requiring cross-section strength checks. Consideration of imperfections and plasticity through stiffness reduction and instability effects through LBA and GNA leads to a more direct and streamlined approach relative to traditional design methods, which utilise a series of indirect methods such as the effective length, notional load concepts and member instability assessment equations. Future research will be directed towards the extension of the proposed approach to planar and space frames made up of prismatic, nonprismatic and curved tubular members and to cold-formed and welded tubular steel members, also covering slender cross-sections.

References

[1] EN 1993-1-1, Eurocode 3 Design of steel structures-Part 1-1: General rules and rules for buildings. European Committee for Standardization (CEN), Brussels; 2005.

[2] AISC 360-16, Specifications for structural steel buildings. American Institute of Steel Construction (AISC), Chicago; 2016.

[3] Standards Australia, AS 4100 steel structures. Australian Building Codes Board, Sydney; 1998.

[4] Zhou, S.P., Chen, W.F.. Design criteria for box columns under biaxial loading. Journal of Structural Engineering, ASCE 1985;111(12):2643–2658.

[5] Chen, W.F., Zhou, S.. C_m factor in Load and Resistance Factor Design. Journal of Structural Engineering, ASCE 1987;113(8):1738–1754.

[6] Liew, J.Y.R., Shanmugam, N., Lee, S.. Design of thin-plated steel box columns under biaxial loading. Journal of Constructional Steel Research 1990;16(1):39–70.

[7] Duan, L., Chen, W.F.. Design interaction equations for cylindrical tubular beam columns. Journal of Structural Engineering, ASCE 1990;116(7):1794–1812.

[8] Shanmugam, N., Liew, J.Y.R., Lee, S.. Ultimate strength design of biaxially loaded steel box beam-columns. Journal of Constructional Steel Research 1993;26(2-3):99–123.

[9] Boissonnade, N., Jaspart, J.P., Muzeau, J.P., Villette, M.. New interaction formulae for beam-columns in Eurocode 3: the French–Belgian approach. Journal of Constructional Steel Research 2004;60(3):421–431.

[10] Greiner, R., Lindner, J.. Interaction formulae for members subjected to bending and axial compression in Eurocode 3 — The method 2 approach. Journal of Constructional Steel Research 2006;62(8):757–770.

[11] Boissonnade, N., Greiner, R., Jaspart, J.P., Lindner, J.. Rules for Member Stability in EN 1993-1-1: Background documentation and design guidelines, No 119. ECCS European Convention for Constructional Steelwork; 2006.

[12] Surovek-Maleck, A.E., White, D.W.. Alternative approaches for elastic analysis and design of steel frames. I: Overview. Journal of Structural Engineering, ASCE 2004;130(8):1186–1196.
[13] Surovek-Maleck, A.E., White, D.W.. Alternative approaches for elastic analysis and design of steel frames. II: Verification studies. Journal of Structural Engineering, ASCE 2004;130(8):1197–1205.
[14] Liew, J.Y.R., Tang, L.. Advanced plastic hinge analysis for the design of tubular space frames. Engineering Structures 2000;22(7):769–783.
[15] White, D.W.. Plastic-hinge methods for advanced analysis of steel frames. Journal of Constructional Steel Research 1993;24(2):121–152.
[16] Kim, S.E., Chen, W.F.. Practical advanced analysis for unbraced steel frame design. Journal of Structural Engineering 1996;122(11):1259–1265.
[17] Kim, S.E., Park, M.H., Choi, S.H.. Practical advanced analysis and design of three-dimensional truss bridges. Journal of Constructional Steel Research 2001;57(8):907–923.
[18] Liew, J.Y.R., Chen, H., Shanmugam, N.E., Chen, W.F.. Improved nonlinear plastic hinge analysis of space frame structures. Engineering Structures 2000;22(10):1324–1338.
[19] Ziemian, R.D., McGuire, W.. Modified tangent modulus approach, a contribution to plastic hinge analysis. Journal of Structural Engineering, ASCE 2002;128(10):1301–1307.
[20] Landesmann, A., Batista, E.M.. Advanced analysis of steel framed buildings using the Brazilian standard and Eurocode-3. Journal of Constructional Steel Research 2005;61(8):1051–1074.
[21] Kucukler, M., Gardner, L., Macorini, L.. A stiffness reduction method for the in-plane design of structural steel elements. Engineering Structures 2014;73:72–84.
[22] Kucukler, M., Gardner, L., Macorini, L.. Development and assessment of a practical stiffness reduction method for the in-plane design of steel frames. Journal of Constructional Steel Research 2016;126:187–200.
[23] Abaqus v.6.14 Reference Manual. Simulia, Dassault Systemes; 2014.
[24] Ofner, R.. Traglasten von stäben aus stahl bei druck und biegung. Ph.D. thesis; TU Graz; 1997.
[25] Kaim, P.. Spatial buckling behaviour of steel members under bending and compression. Ph.D. thesis; TU Graz; 2004.
[26] Taras, A.. Contribution to the development of consistent stability design rules for steel members. Ph.D. thesis; TU Graz; 2010.
[27] ECCS, Ultimate limit state calculation of sway frames with rigid joints. Tech. Rep.; No. 33, Technical Committee 8 (TC 8) of European Convention for Constructional Steelwork (ECCS); 1984.
[28] Yun, X., Gardner, L.. Stress-strain curves for hot-rolled steels. Journal of Constructional Steel Research 2017;133:36–46.
[29] Zubydan, A.H.. A simplified model for inelastic second order analysis of planar frames. Engineering Structures 2010;32(10):3258–3268.
[30] Duan, L., Chen, W.F.. A yield surface equation for doubly symmetrical sections. Engineering Structures 1990;12(2):114–119.
[31] Kucukler, M., Gardner, L., Macorini, L.. Lateral–torsional buckling assessment of steel beams through a stiffness reduction method. Journal of Constructional Steel Research 2015;109:87–100.
[32] Kucukler, M., Gardner, L., Macorini, L.. Flexural–torsional buckling assessment of steel beam–columns through a stiffness reduction method. Engineering Structures 2015;101:662–676.
[33] Johnston, B.G.. Guide to design criteria for metal compression members, Second Edition. Wiley; 1966.
[34] Orbison, J.G.. Nonlinear static analysis of three-dimensional steel frames. Ph.D. thesis; Cornell University; 1982.
[35] Liew, J.R., White, D.W., Chen, W.F.. Second-order refined plastic-hinge analysis for frame design. part i. Journal of Structural Engineering, ASCE 1993;119(11):3196–3216.
[36] Kucukler, M.. Stiffness reduction approach for structural steel design. Ph.D. thesis; Imperial College London; 2015.
[37] EN 1993-1-5, Eurocode 3 Design of steel structures-Part 1-5: Plated structural elements. European Committee for Standardization (CEN), Brussels; 2005.
[38] Goncalves, R., Camotim, D.. On the application of beam-column interaction formulae to steel members with arbitrary loading and support conditions. Journal of Constructional Steel Research 2004;60(3):433–450.

Figures captions

Figure 1 : Material stress-strain curves used in finite element models

Figure 2 : Residual stress patterns applied to the finite element models (+ve tension, -ve compression)

Figure 3 : Application of geometrical imperfections to finite element models using the lowest buckling modes about the principal axes

Figure 4 : Derivation of stiffness reduction function under bending τ_M considering the moment-curvature relationship of a cross-section subjected to biaxial bending

Figure 5 : Stiffness reduction functions τ_{My} and τ_{Mz} for tubular sections under different levels of biaxial bending

Figure 6 : Stiffness reduction functions used for different stiffness reduction methods (SRM) proposed in this study for a member with an SHS 100×5 profile and subjected to monoaxial bending plus $M_{y,Ed}$ axial compression N_{Ed}

Figure 7 : Assessment of accuracy of the proposed stiffness reduction approaches against GMNIA and Eurocode 3 [1] Annex A and Annex B beam-column design methods for laterally-restrained tubular beam-columns subjected to axial compression plus uniform monoaxial bending

Figure 8 : Determination of radial errors ϵ used to assess the accuracy of the proposed stiffness reduction approaches

Figure 9 : Accuracy of the proposed stiffness reduction approaches against GMNIA and Eurocode 3 Annex A and Annex B beam-column design methods for laterally-restrained tubular beam-columns subjected to axial compression plus varying monoaxial bending

Figure 10 : Accuracy of the proposed stiffness reduction approaches against GMNIA and Eurocode 3 Annex A and Annex B beam-column design methods for laterally-restrained tubular beam-columns with elastic rotational end restraints

Figure 11 : Accuracy of the proposed stiffness reduction method against GMNIA and Eurocode 3 Annex A and Annex B beam-column design methods for laterally-unrestrained tubular beam-columns subjected to axial compression plus uniform monoaxial bending

Figure 12 : Accuracy assessment of the proposed stiffness reduction approaches against GMNIA and Eurocode 3 Annex A and Annex B beam-column design methods for tubular beam-columns with an RHS $200 \times 100 \times 10$ cross-section subjected to axial compression plus uniform biaxial bending

Figure 13 : Accuracy assessment of the proposed stiffness reduction approaches against GMNIA for tubular beam-columns with a CHS 114.3×3.6 cross-section subjected to axial compression plus uniform biaxial bending

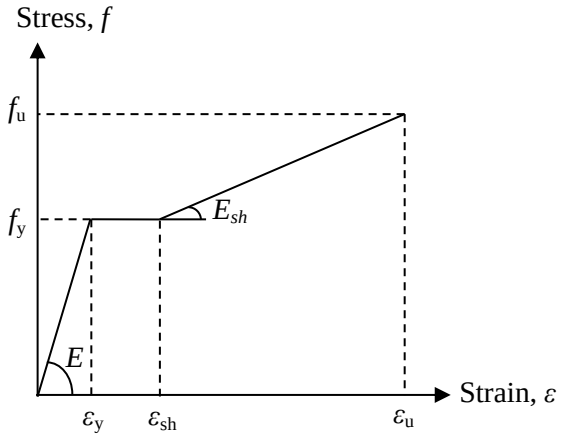

Figure 1: Material stress-strain curves used in finite element models

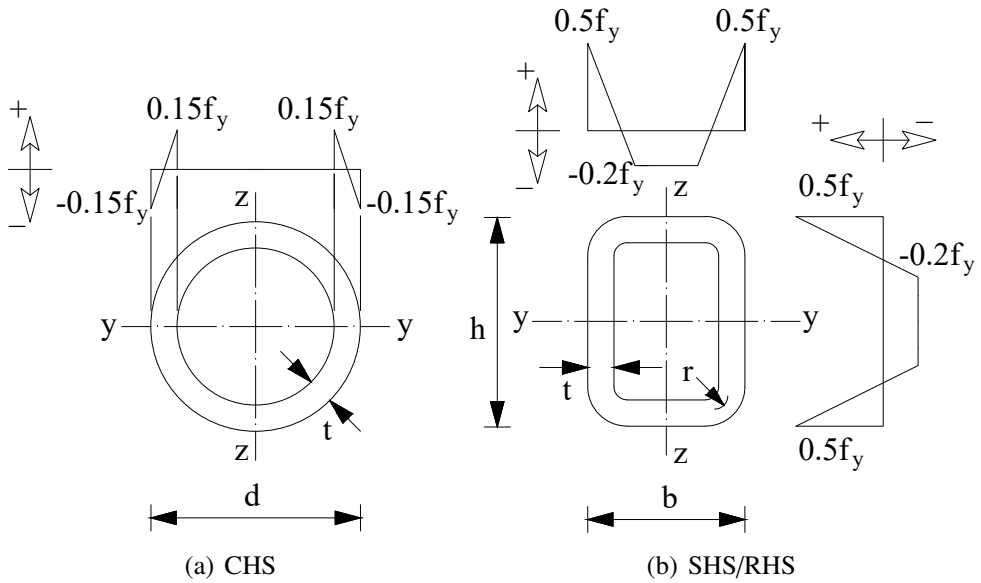

(a) CHS (b) SHS/RHS

Figure 2: Residual stress patterns applied to the finite element models (+ve tension, -ve compression)

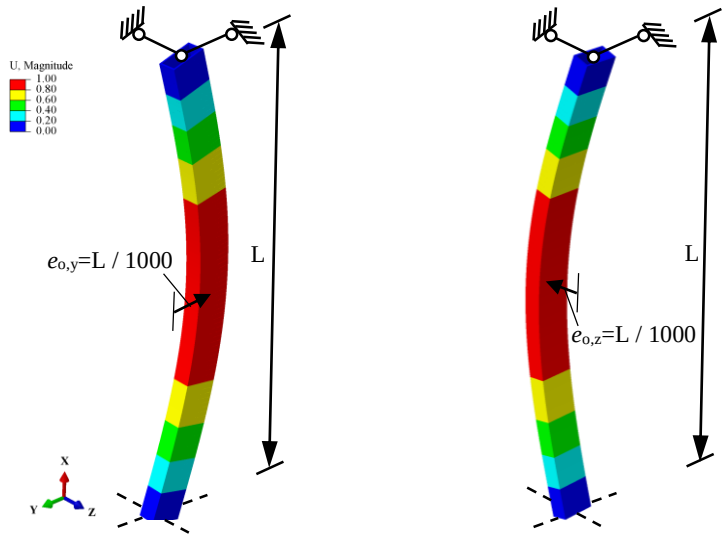

Figure 3: Application of geometrical imperfections to finite element models using the lowest buckling modes about the principal axes

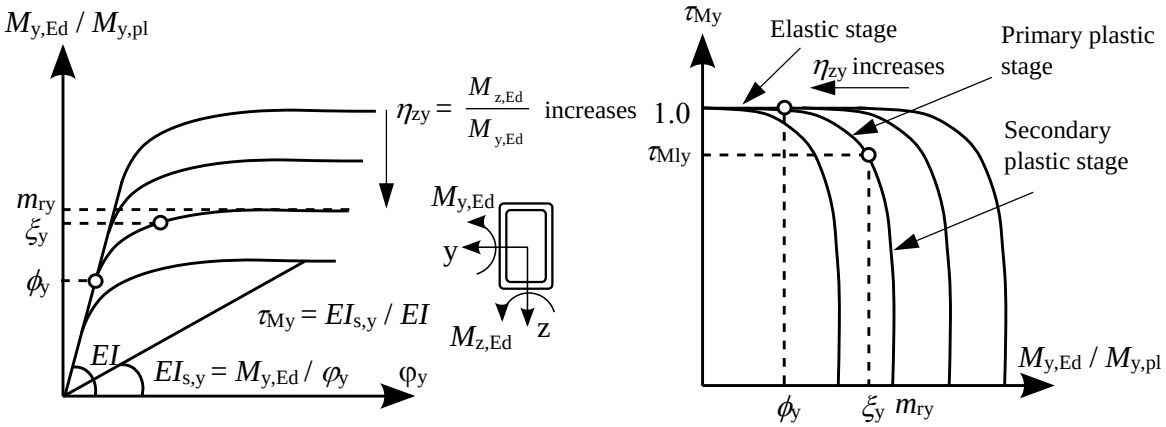

(a) Moment-curvature relationship

(b) Stiffness reduction

Figure 4: Derivation of stiffness reduction function under bending τ_M considering the moment-curvature relationship of a cross-section subjected to biaxial bending

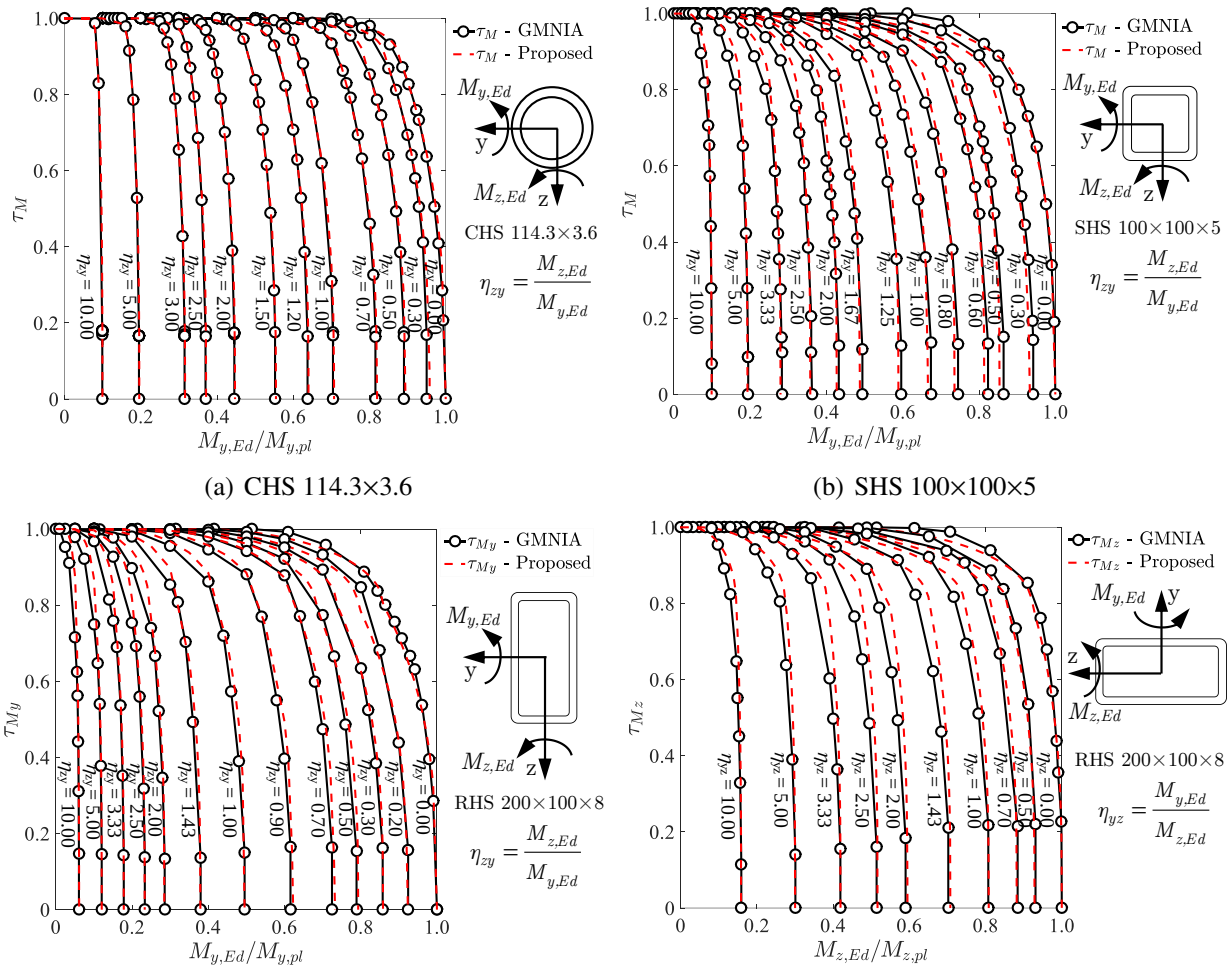

(a) CHS 114.3×3.6

(b) SHS 100×100×5

(c) RHS 200×100×8

(d) RHS 200×100×8

Figure 5: Stiffness reduction functions τ_{My} and τ_{Mz} for tubular sections under different levels of biaxial bending

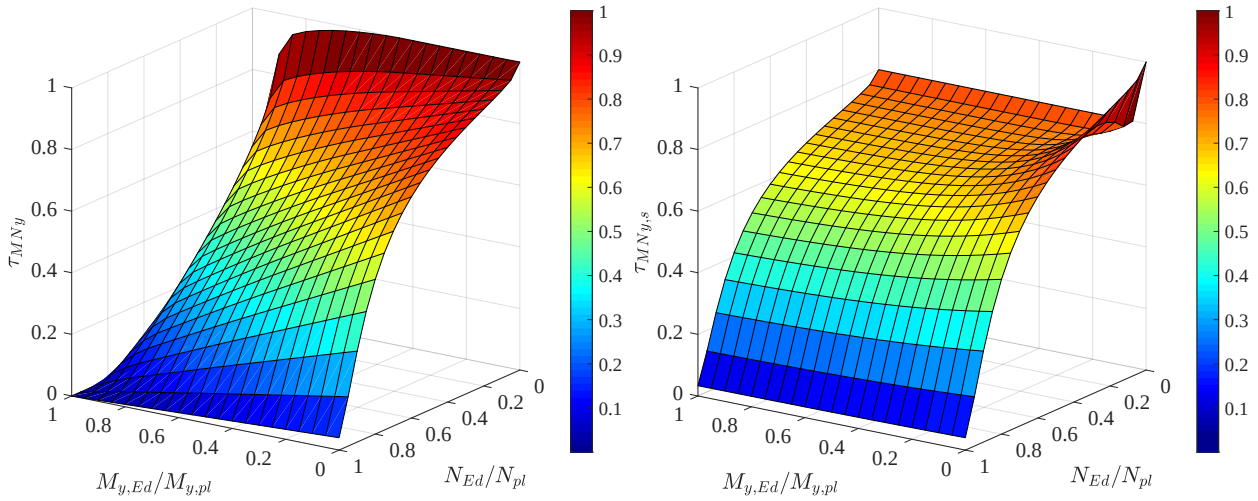

(a) SRM (τ_{MNy})

(b) SRM – Simplified ($\tau_{MNy,s}$)

Figure 6: Stiffness reduction functions used for different stiffness reduction methods (SRM) proposed in this study for a member with an SHS 100×5 profile and subjected to monoaxial bending plus $M_{y,Ed}$ axial compression N_{Ed}

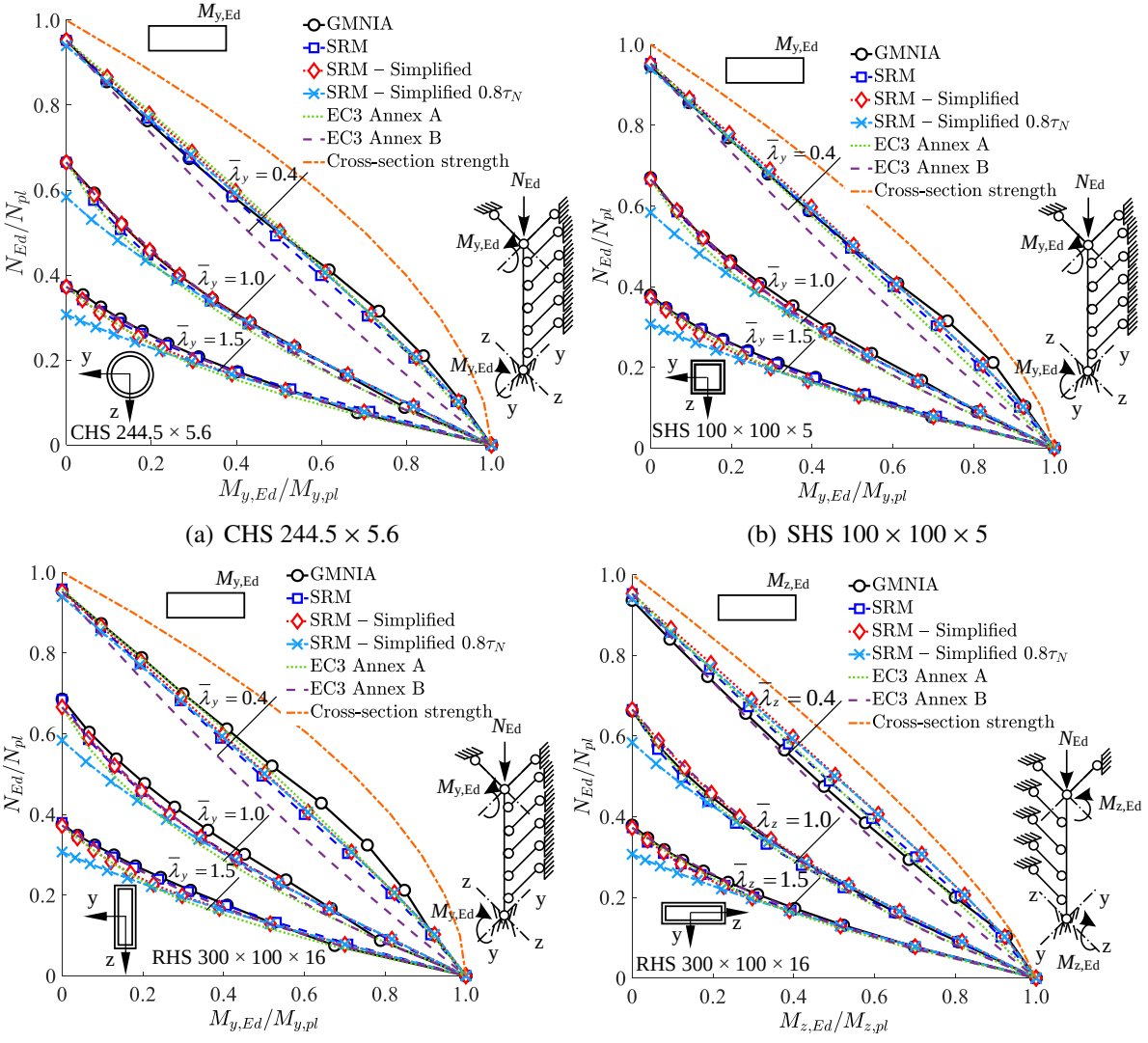

(a) CHS 244.5 × 5.6

(b) SHS 100 × 100 × 5

(c) RHS 300 × 100 × 16 - major

(d) RHS 300 × 100 × 16 - minor

Figure 7: Assessment of accuracy of the proposed stiffness reduction approaches against GMNIA and Eurocode 3 [1] Annex A and Annex B beam-column design methods for laterally-restrained tubular beam-columns subjected to axial compression plus uniform monoaxial bending

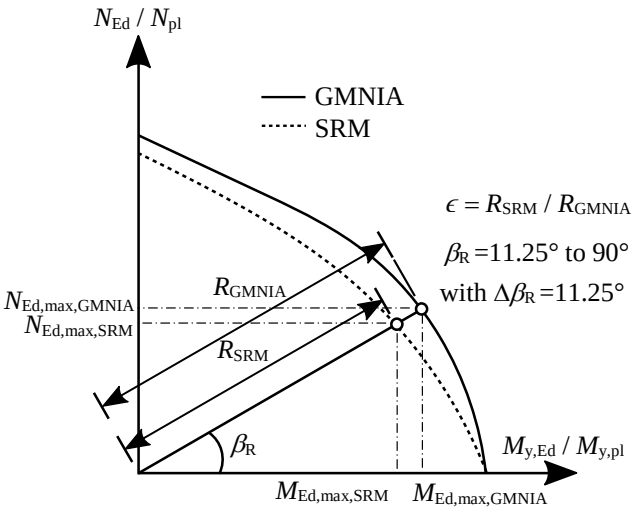

Figure 8: Determination of radial errors ϵ used to assess the accuracy of the proposed stiffness reduction approaches

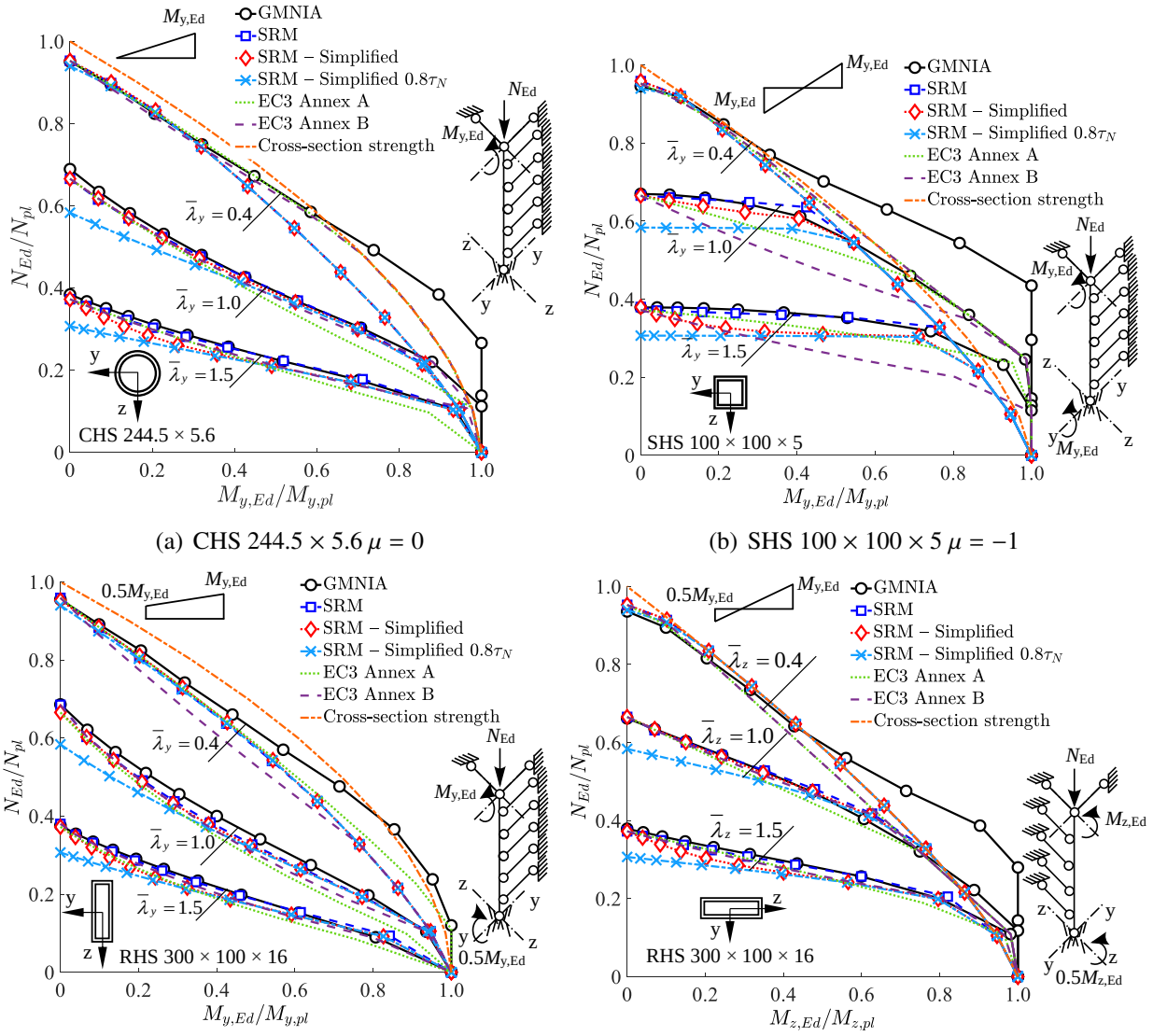

(a) CHS 244.5 × 5.6 $\mu = 0$

(b) SHS 100 × 100 × 5 $\mu = -1$

(c) RHS 300 × 100 × 16 - major $\mu = 0.5$

(d) RHS 300 × 100 × 16 - minor $\mu = -0.5$

Figure 9: Accuracy of the proposed stiffness reduction approaches against GMNIA and Eurocode 3 Annex A and Annex B beam-column design methods for laterally-restrained tubular beam-columns subjected to axial compression plus varying monoaxial bending

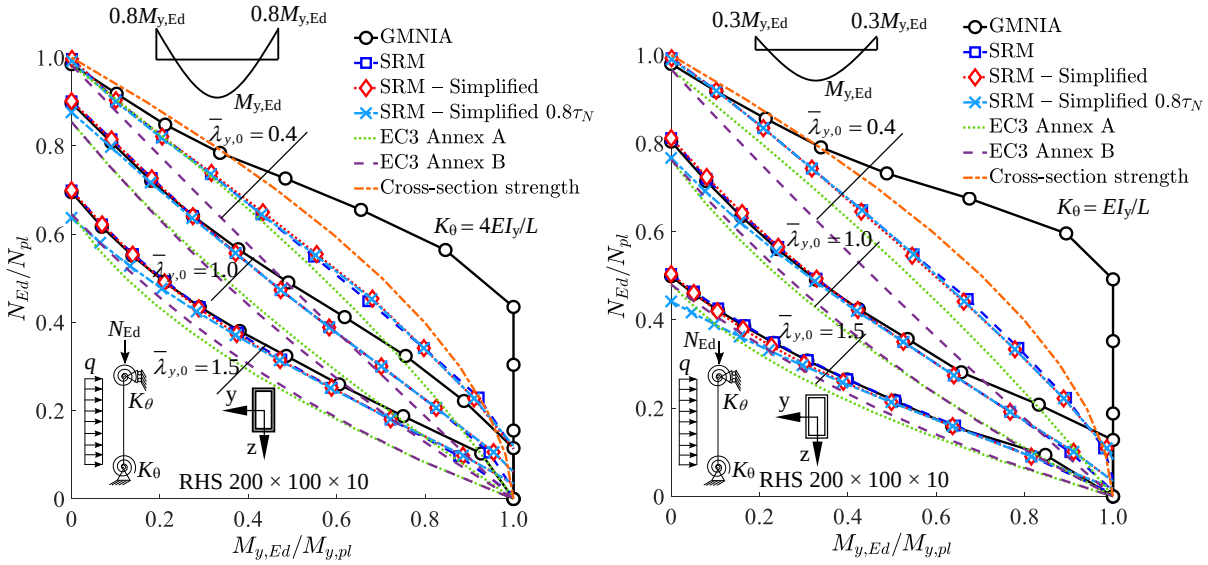

(a) $K_\theta = 4EI_y/L$ (b) $K_\theta = EI_y/L$

Figure 10: Accuracy of the proposed stiffness reduction approaches against GMNIA and Eurocode 3 Annex A and Annex B beam-column design methods for laterally-restrained tubular beam-columns with elastic rotational end restraints

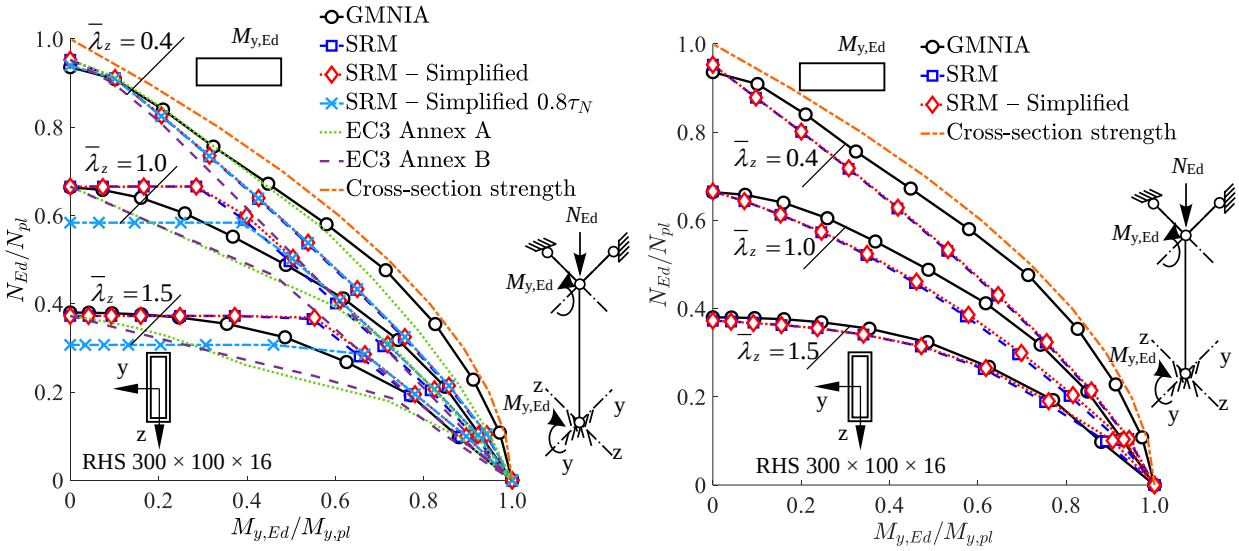

(a) Pre-buckling effects neglected in the SRM (b) Pre-buckling effects considered in the SRM

Figure 11: Accuracy of the proposed stiffness reduction method against GMNIA and Eurocode 3 Annex A and Annex B beam-column design methods for laterally-unrestrained tubular beam-columns subjected to axial compression plus uniform monoaxial bending

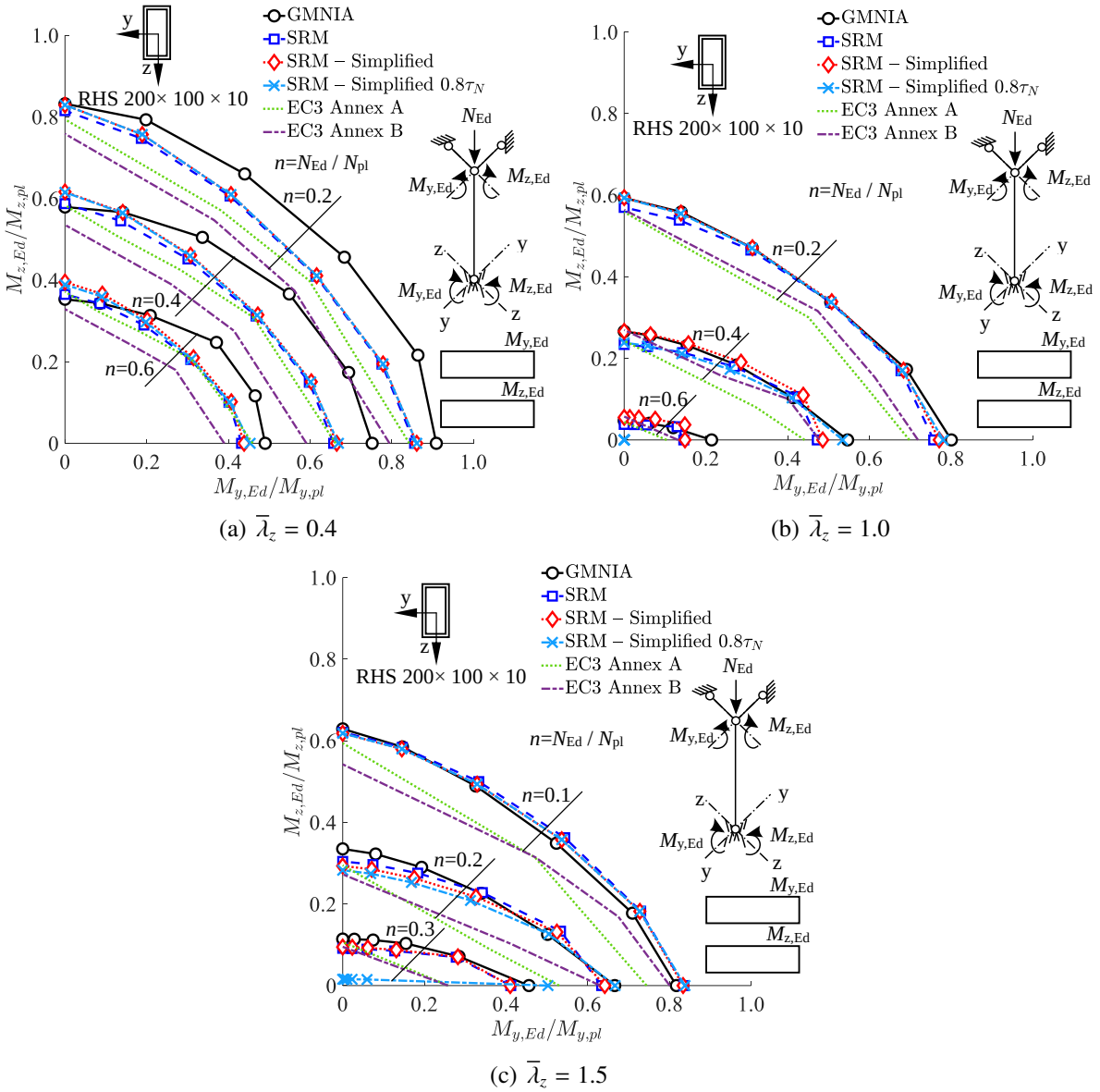

(a) $\overline{\lambda}_z$ = 0.4

(b) $\overline{\lambda}_z$ = 1.0

(c) $\overline{\lambda}_z$ = 1.5

Figure 12: Accuracy assessment of the proposed stiffness reduction approaches against GMNIA and Eurocode 3 Annex A and Annex B beam-column design methods for tubular beam-columns with an RHS 200 × 100 × 10 cross-section subjected to axial compression plus uniform biaxial bending

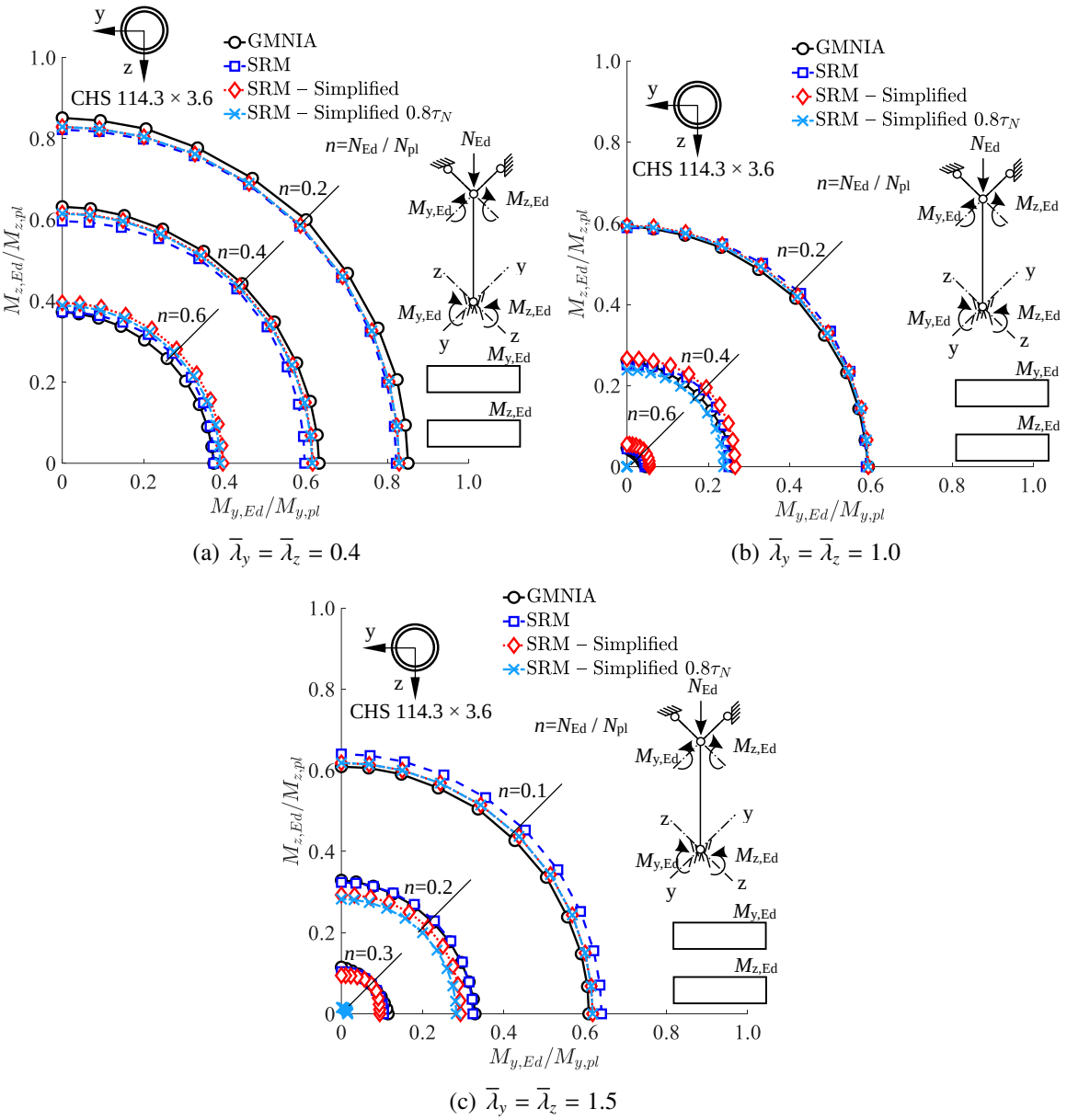

(a) $\overline{\lambda}_y = \overline{\lambda}_z = 0.4$

(b) $\overline{\lambda}_y = \overline{\lambda}_z = 1.0$

(c) $\overline{\lambda}_y = \overline{\lambda}_z = 1.5$

Figure 13: Accuracy assessment of the proposed stiffness reduction approaches against GMNIA for tubular beam-columns with a CHS 114.3 × 3.6 cross-section subjected to axial compression plus uniform biaxial bending

Tables captions

Table 1 : Range of considered CHS, SHS and RHS

Table 2 : Parameters for the stiffness reduction function for tubular sections under biaxial bending τ_{My} used to reduce major axis flexural stiffness EI_y

Table 3 : Parameters for the stiffness reduction function for tubular sections under biaxial bending τ_{Mz} used to reduce minor axis flexural stiffness EI_z

Table 4 : Auxiliary coefficients of the stiffness reduction function for combined bending and axial compression

Table 5 : Accuracy of the proposed stiffness reduction approaches relative to Eurocode 3 for tubular beam-columns subjected to axial compression plus uniform monoaxial bending

Table 6 : Accuracy of the proposed stiffness reduction approaches relative to Eurocode 3 for CHS beam-columns subjected to axial compression plus varying monoaxial bending

Table 7 : Accuracy of the proposed stiffness reduction approaches relative to Eurocode 3 for RHS beam-columns subjected to axial compression plus varying major axis monoaxial bending

Table 8 : Accuracy of the proposed stiffness reduction approaches relative to Eurocode 3 for RHS beam-columns subjected to axial compression plus varying minor axis monoaxial bending

Table 9 : Accuracy of the proposed stiffness reduction method in comparison to GMNIA and Eurocode 3 Annex A and Annex B beam-column design methods for beam-columns with RHS 200×100×10 section subjected to biaxial bending plus axial compression

Table 1: Range of considered CHS, SHS and RHS

	CHS	SHS/RHS		
	d/t	h/t	b/t	h/b
Maximum	72.54	42.25	35.21	3.00
Minimum	6.66	9.52	4.80	1.00

Table 2: Parameters for the stiffness reduction function for tubular sections under biaxial bending τ_{My} used to reduce major axis flexural stiffness EI_y

Cross-section	τ_{Mly}	ϕ_y	m_{ry}	ξ_{my}	β_{my}	δ_{my}
CHS	0.90	$\frac{0.85W_{el,y}}{W_{pl,y}\sqrt{1+\eta_{zy}^2}}$	$\frac{1}{\sqrt{1+\eta_{zy}^2}}$	$m_{ry}/1.14$	2.0	2.7
SHS	0.80	$\frac{0.5W_{el,y}}{W_{pl,y}(1+\eta_{zy})}$	$\left[\frac{1}{1+\eta_{zy}^{1.7}}\right]^{1/1.7}$	$0.89m_{ry}$	2.0	3.0
RHS	0.80	$\frac{0.5W_{el,y}}{W_{pl,y}\left(1+\frac{\eta_{zy}W_{el,y}}{W_{el,z}}\right)}$	$\left[\frac{1}{1+\left(\frac{\eta_{zy}W_{pl,y}}{W_{pl,z}}\right)^{1.7}}\right]^{1/1.7}$	$0.89m_{ry}(h/b)^{-0.05}$	2.0	3.0

Table 3: Parameters for the stiffness reduction function for tubular sections under biaxial bending τ_{Mz} used to reduce minor axis flexural stiffness EI_z

Cross-section	τ_{Mlz}	ϕ_z	m_{rz}	ξ_{mz}	β_{mz}	δ_{mz}
CHS	0.90	$\frac{0.85W_{el,z}}{W_{pl,z}\sqrt{1+\eta_{yz}^2}}$	$\frac{1}{\sqrt{1+\eta_{yz}^2}}$	$m_{rz}/1.14$	2.0	2.7
SHS	0.80	$\frac{0.5W_{el,z}}{W_{pl,z}(1+\eta_{yz})}$	$\left[\frac{1}{1+\eta_{yz}^{1.7}}\right]^{1/1.7}$	$0.89m_{rz}$	2.0	3.0
RHS	0.80	$\frac{0.5W_{el,z}}{W_{pl,z}\left(1+\frac{\eta_{yz}W_{el,z}}{W_{el,y}}\right)}$	$\left[\frac{1}{1+\left(\frac{\eta_{yz}W_{pl,z}}{W_{pl,y}}\right)^{1.7}}\right]^{1/1.7}$	$0.89m_{rz}(b/h)^{-0.05}$	2.0	3.0

Table 4: Auxiliary coefficients of the stiffness reduction function for combined bending and axial compression

Cross-section	η_y	ρ_y	η_z	ρ_z
CHS	0.70	0.80	0.70	0.80
SHS	0.70	1.00	0.70	1.00
RHS	0.70	1.00	0.60	0.70

Table 5: Accuracy of the proposed stiffness reduction approaches relative to Eurocode 3 for tubular beam-columns subjected to axial compression plus uniform monoaxial bending

	Loading conditions	$\overline{\lambda}$	N	ϵ_{av}	ϵ_{COV}	ϵ_{max}	ϵ_{min}
SRM	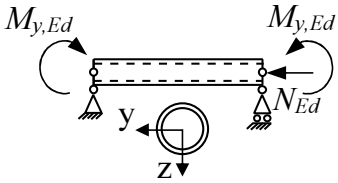	$\overline{\lambda}_y$=0.4, 1.0, 1.5	210	0.99	0.018	1.05	0.96
SRM - Simplified				0.99	0.024	1.03	0.95
SRM - Simplified $0.8\tau_N$				0.96	0.063	1.03	0.80
EC 3 Annex A				0.98	0.034	1.07	0.91
EC 3 Annex B				0.98	0.031	1.02	0.90
SRM	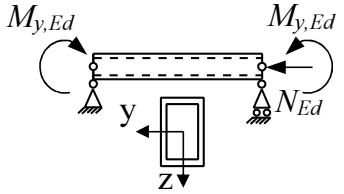	$\overline{\lambda}_y$=0.4, 1.0, 1.5	210	0.99	0.022	1.05	0.93
SRM - Simplified				0.99	0.026	1.04	0.93
SRM - Simplified $0.8\tau_N$				0.94	0.055	1.04	0.81
EC 3 Annex A				0.96	0.030	1.01	0.90
EC 3 Annex B				0.97	0.036	1.02	0.88
SRM	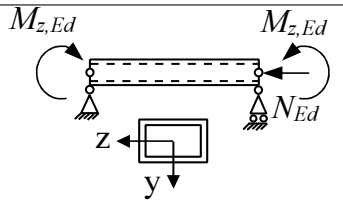	$\overline{\lambda}_z$=0.4, 1.0, 1.5	210	0.98	0.023	1.03	0.94
SRM - Simplified				1.00	0.028	1.06	0.94
SRM - Simplified $0.8\tau_N$				0.96	0.063	1.06	0.80
EC 3 Annex A				0.98	0.027	1.06	0.93
EC 3 Annex B				0.99	0.026	1.04	0.90

Table 6: Accuracy of the proposed stiffness reduction approaches relative to Eurocode 3 for CHS beam-columns subjected to axial compression plus varying monoaxial bending

	Loading conditions	$\overline{\lambda}$	N	ϵ_{av}	ϵ_{COV}	ϵ_{max}	ϵ_{min}
SRM	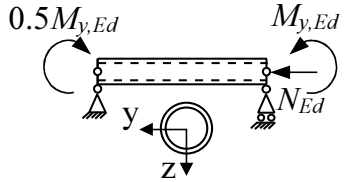	$\overline{\lambda}_y$=0.4, 1.0, 1.5	196	0.99	0.022	1.04	0.92
SRM - Simplified				0.98	0.028	1.02	0.92
SRM - Simplified $0.8\tau_N$				0.94	0.065	1.02	0.80
EC 3 Annex A				0.97	0.031	1.05	0.92
EC 3 Annex B				0.97	0.022	1.01	0.92
SRM	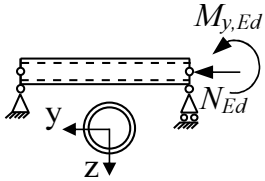	$\overline{\lambda}_y$=0.4, 1.0, 1.5	160	0.99	0.017	1.02	0.92
SRM - Simplified				0.97	0.029	1.01	0.92
SRM - Simplified $0.8\tau_N$				0.93	0.063	1.00	0.80
EC 3 Annex A				0.97	0.027	1.04	0.91
EC 3 Annex B				0.98	0.014	1.04	0.95
SRM	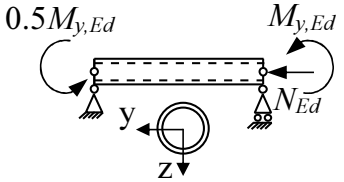	$\overline{\lambda}_y$=0.4, 1.0, 1.5	154	0.99	0.023	1.03	0.93
SRM - Simplified				0.96	0.034	1.01	0.89
SRM - Simplified $0.8\tau_N$				0.91	0.071	1.00	0.80
EC 3 Annex A				0.97	0.022	1.02	0.92
EC 3 Annex B				0.98	0.027	1.04	0.94
SRM	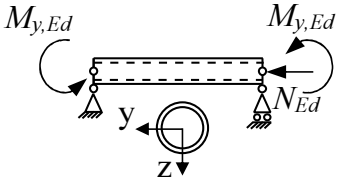	$\overline{\lambda}_y$=0.4, 1.0, 1.5	127	0.98	0.032	1.05	0.94
SRM - Simplified				0.95	0.052	1.02	0.85
SRM - Simplified $0.8\tau_N$				0.89	0.088	1.02	0.80
EC 3 Annex A				0.96	0.033	1.04	0.91
EC 3 Annex B				0.90	0.076	1.01	0.78

Table 7: Accuracy of the proposed stiffness reduction approaches relative to Eurocode 3 for RHS beam-columns subjected to axial compression plus varying major axis monoaxial bending

	Loading conditions	$\overline{\lambda}$	N	ϵ_{av}	ϵ_{COV}	ϵ_{max}	ϵ_{min}
SRM	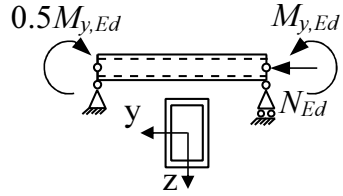	$\overline{\lambda}_y$=0.4, 1.0, 1.5	189	0.99	0.020	1.05	0.92
SRM - Simplified				0.97	0.029	1.03	0.92
SRM - Simplified $0.8\tau_N$				0.93	0.059	1.03	0.81
EC 3 Annex A				0.95	0.031	1.01	0.90
EC 3 Annex B				0.97	0.029	1.02	0.89
SRM	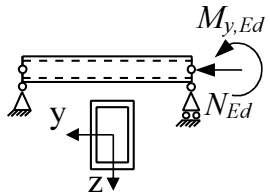	$\overline{\lambda}_y$=0.4, 1.0, 1.5	175	0.99	0.020	1.03	0.91
SRM - Simplified				0.96	0.029	1.01	0.90
SRM - Simplified $0.8\tau_N$				0.92	0.058	1.01	0.81
EC 3 Annex A				0.96	0.035	1.01	0.89
EC 3 Annex B				0.97	0.027	1.05	0.93
SRM	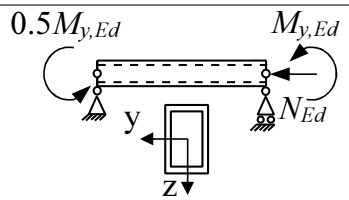	$\overline{\lambda}_y$=0.4, 1.0, 1.5	149	0.99	0.018	1.02	0.93
SRM - Simplified				0.96	0.035	1.02	0.89
SRM - Simplified $0.8\tau_N$				0.91	0.062	1.00	0.81
EC 3 Annex A				0.96	0.032	1.03	0.91
EC 3 Annex B				0.97	0.029	1.05	0.91
SRM	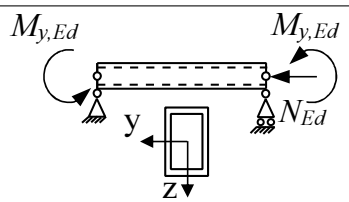	$\overline{\lambda}_y$=0.4, 1.0, 1.5	127	0.99	0.023	1.04	0.91
SRM - Simplified				0.95	0.047	1.02	0.86
SRM - Simplified $0.8\tau_N$				0.89	0.075	1.00	0.81
EC 3 Annex A				0.96	0.034	1.05	0.90
EC 3 Annex B				0.90	0.082	1.01	0.75

Table 8: Accuracy of the proposed stiffness reduction approaches relative to Eurocode 3 for RHS beam-columns subjected to axial compression plus varying minor axis monoaxial bending

	Loading conditions	$\overline{\lambda}$	N	ϵ_{av}	ϵ_{COV}	ϵ_{max}	ϵ_{min}
SRM	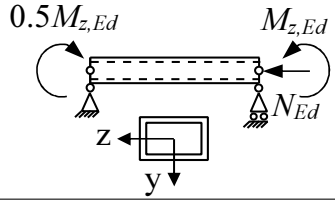	$\overline{\lambda}_z$=0.4, 1.0, 1.5	161	0.99	0.023	1.04	0.95
SRM - Simplified				0.99	0.030	1.06	0.93
SRM - Simplified $0.8\tau_N$				0.95	0.066	1.05	0.80
EC 3 Annex A				0.97	0.033	1.05	0.90
EC 3 Annex B				0.99	0.019	1.03	0.94
SRM	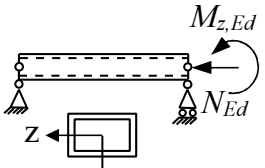	$\overline{\lambda}_z$=0.4, 1.0, 1.5	144	0.99	0.018	1.03	0.96
SRM - Simplified				0.98	0.031	1.03	0.92
SRM - Simplified $0.8\tau_N$				0.94	0.068	1.03	0.80
EC 3 Annex A				0.97	0.031	1.02	0.90
EC 3 Annex B				0.99	0.019	1.04	0.94
SRM	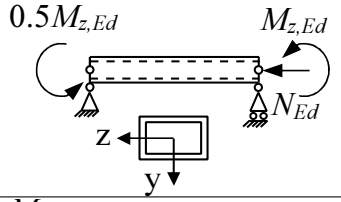	$\overline{\lambda}_z$=0.4, 1.0, 1.5	129	0.99	0.020	1.03	0.89
SRM - Simplified				0.98	0.038	1.03	0.89
SRM - Simplified $0.8\tau_N$				0.93	0.073	1.03	0.80
EC 3 Annex A				0.97	0.026	1.03	0.91
EC 3 Annex B				0.98	0.024	1.06	0.92
SRM	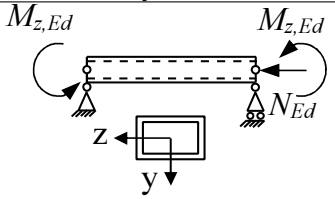	$\overline{\lambda}_z$=0.4, 1.0, 1.5	113	0.98	0.035	1.05	0.84
SRM - Simplified				0.96	0.054	1.05	0.84
SRM - Simplified $0.8\tau_N$				0.91	0.079	1.05	0.80
EC 3 Annex A				0.97	0.030	1.02	0.87
EC 3 Annex B				0.92	0.076	1.02	0.77

Table 9: Accuracy of the proposed stiffness reduction method in comparison to GMNIA and Eurocode 3 Annex A and Annex B beam-column design methods for beam-columns with RHS 200×100×10 section subjected to biaxial bending plus axial compression

	Loading conditions	$\overline{\lambda}$	N	ϵ_{av}	ϵ_{COV}	ϵ_{max}	ϵ_{min}
SRM	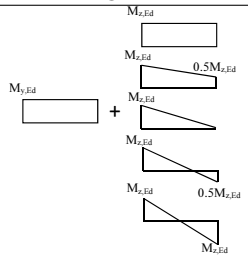	$\overline{\lambda}_z$=0.4, 1.0, 1.5	235	0.96	0.049	1.06	0.81
SRM (no pre-buckl.)				0.98	0.054	1.09	0.81
SRM - Simplified				0.96	0.056	1.04	0.74
SRM - Simplified (no pre-buckl.)				0.97	0.062	1.08	0.74
SRM - Simplified 0.8τ_N				0.95	0.086	1.07	0.62
EC 3 Annex A				0.88	0.094	1.01	0.61
EC 3 Annex B				0.89	0.105	1.04	0.47
SRM	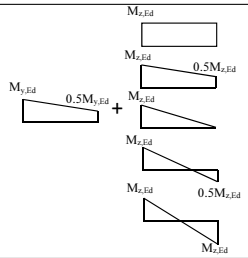	$\overline{\lambda}_z$=0.4, 1.0, 1.5	203	0.96	0.054	1.07	0.80
SRM (no pre-buckl.)				0.97	0.060	1.10	0.80
SRM - Simplified				0.95	0.061	1.06	0.74
SRM - Simplified (no pre-buckl.)				0.97	0.068	1.09	0.74
SRM - Simplified 0.8τ_N				0.93	0.093	1.07	0.60
EC 3 Annex A				0.87	0.099	1.01	0.63
EC 3 Annex B				0.89	0.120	1.04	0.47
SRM	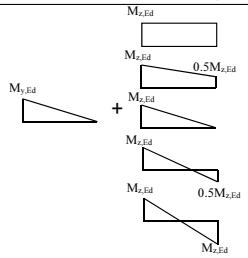	$\overline{\lambda}_z$=0.4, 1.0, 1.5	175	0.95	0.055	1.06	0.84
SRM (no pre-buckl.)				0.97	0.057	1.09	0.84
SRM - Simplified				0.94	0.065	1.05	0.74
SRM - Simplified (no pre-buckl.)				0.96	0.068	1.07	0.74
SRM - Simplified 0.8τ_N				0.92	0.104	1.05	0.53
EC 3 Annex A				0.89	0.092	1.01	0.68
EC 3 Annex B				0.89	0.132	1.04	0.47
SRM	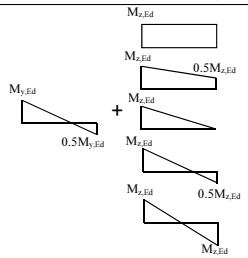	$\overline{\lambda}_z$=0.4, 1.0, 1.5	156	0.94	0.064	1.06	0.80
SRM (no pre-buckl.)				0.95	0.058	1.06	0.80
SRM - Simplified				0.93	0.077	1.05	0.73
SRM - Simplified (no pre-buckl.)				0.94	0.073	1.05	0.73
SRM - Simplified 0.8τ_N				0.90	0.124	1.05	0.46
EC 3 Annex A				0.90	0.085	1.01	0.70
EC 3 Annex B				0.89	0.125	1.04	0.47
SRM	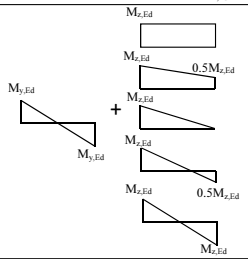	$\overline{\lambda}_z$=0.4, 1.0, 1.5	137	0.95	0.062	1.05	0.77
SRM (no pre-buckl.)				0.95	0.059	1.05	0.77
SRM - Simplified				0.94	0.079	1.05	0.71
SRM - Simplified (no pre-buckl.)				0.94	0.077	1.05	0.71
SRM - Simplified 0.8τ_N				0.90	0.135	1.05	0.41
EC 3 Annex A				0.90	0.080	1.01	0.71
EC 3 Annex B				0.88	0.137	1.04	0.47